NASA TECHNICAL NOTE

NASA TN D-7978

NASA TN D-7978

~~A~~ 4. SHORT STATIC-PRESSURE PROBE DESIGN FOR SUPERSONIC FLOW

S. Z. Pinckney

Langley Research Center
Hampton, Va. 23665

NATIONAL AERONAUTICS AND SPACE ADMINISTRATION • WASHINGTON, D. C. • JULY 1975

1. Report No. NASA TN D-7978	2. Government Accession No.	3. Recipient's Catalog No.
4. Title and Subtitle A SHORT STATIC-PRESSURE PROBE DESIGN FOR SUPERSONIC FLOW		5. Report Date July 1975 6. Performing Organization Code
7. Author(s) S. Z. Pinckney		8. Performing Organization Report No. L-10033
9. Performing Organization Name and Address NASA Langley Research Center Hampton, Va. 23665		10. Work Unit No. 505-05-41-01 11. Contract or Grant No.
12. Sponsoring Agency Name and Address National Aeronautics and Space Administration Washington, D.C. 20546		13. Type of Report and Period Covered Technical Note 14. Sponsoring Agency Code

15. Supplementary Notes

16. Abstract

A static-pressure probe design concept has been developed which has the static holes located close to the probe tip and is relatively insensitive to probe angle of attack and circumferential static hole location. Probes were constructed with 10° and 20° half-angle cone tips followed by a tangent conic curve section and a tangent cone section of 2°, 3°, or 3.5°, and were tested at Mach numbers of 2.5 and 4.0 and angles of attack up to 12°. Experimental results indicated that for stream Mach numbers of 2.5 and 4.0 and probe angle of attack within $\pm 10^{\circ}$, values of stream static pressure can be determined from probe calibration to within about ±4 percent. If the probe is alined within about 7° of the flow experimental results indicated, the stream static pressures can be determined to within 2 percent from probe calibration.

17. Key Words (Suggested by Author(s)) Supersonic flow Static-pressure probe	18. Distribution Statement Unclassified – Unlimited New Subject Category 34		
19. Security Classif. (of this report) Unclassified	20. Security Classif. (of this page) Unclassified	21. No. of Pages 37	22. Price* $3.75

*For sale by the National Technical Information Service, Springfield, Virginia 22151

A SHORT STATIC-PRESSURE PROBE DESIGN FOR SUPERSONIC FLOW

S. Z. Pinckney
Langley Research Center

SUMMARY

A static probe design concept has been developed which has the static holes located close to the probe tip and is relatively insensitive to probe angle of attack and circumferential static hole location. Probes were constructed with 10° and 20° half-angle cone tips followed by a tangent conic curve section and a tangent cone section of 2°, 3°, or 3.5°, and were tested at Mach numbers 2.5 and 4.0 and angles of attack up to 12°. The results of the tests indicate the following:

(1) The construction of the probes was not difficult with standard shop techniques.

(2) For stream Mach numbers of 2.5 and 4.0 and probe angle of attack (angle between stream flow direction and probe center line) within $\pm 10^{\circ}$, values of stream static pressure can be determined from the probe calibration to within about ± 4 percent.

(3) If the probe is alined within about 7° of the flow, then the stream static pressures can be determined to within 2 percent from probe calibration.

(4) For an angle of attack of 0°, good comparisons are obtained between theoretical predictions of probe static pressure and experimental probe calibrations.

(5) Theoretical predictions indicate that a probe of the present design with a 10° cone half-angle tip and a 1.5° half-angle tangent cone would be the least sensitive to Mach number.

INTRODUCTION

Static-pressure probes for measuring instream static pressure in supersonic flows in tunnels and over models have been the subject of much design and development effort. Success has been achieved in the development of a static-pressure probe which gives accurate measurements in flows where the probe is alined parallel to the flow (refs. 1 to 3), and where the distance between flow discontinuities (such as shocks) is larger than the distance between the probe tip and static-pressure holes. These conditions are usually met in the large tunnels. This static-pressure probe design, from references 1 and 2, consists of a conical tip followed by a cylindrical tube section in which four static holes are located at 90° intervals about the cylindrical tube and 10 tube diameters or greater

downstream of the cone tip; this type of probe could typically be as short as 1 centimeter. For the case of flow measurements in nozzle and inlet model throats, however, as well as in many model flow fields, variations of static pressure and flow direction frequently occur in dimensions less than 1 centimeter. Use of this conventional static-pressure probe in such cases results in the static holes not being in the same flow environment as the tip, and the measurement accuracy could be thereby degraded. At angle of attack, where flow differences between tip and holes are accentuated, additional inaccuracies in static-pressure measurements are introduced through use of this type of probe. Many attempts have been made to improve probe incidence characteristics through the use of special probe tip shapes and sensing hole locations. (See refs. 4 to 6.) In these investigations it was usual to locate two sensing holes symmetrically with respect to a particular angle-of-attack plane; however, when the probe is rotated relative to this angle-of-attack plane, the measurement deteriorates rapidly.

In reference 7, Clippinger and Giese used the method of characteristics to study the zero incidence flow about cone-cylinders at supersonic speeds. Experimental verification of a suggested short probe based on this theoretical investigation is demonstrated by the short probe (probe design based on investigations of refs. 7 and 8) tested in reference 9. This probe is 0.0508 meter in diameter and has 24 static holes located symmetrically about the cylinder. Favorable results were obtained for Mach numbers 1.4 to 2.5 and angles of attack up to 18° ($\pm$3-percent variation). If this 0.0508-meter-diameter probe is scaled down to the size required to survey nozzle and inlet flows (about 0.001524-meter diameter or smaller), the static hole sizes would not be realistic. This large number of static holes is a result of attempting to reduce circumferential static hole-location effects and it is not known whether the number of static holes could be reduced and still obtain the satisfactory characteristics shown by this probe. The results of another attempt to design a static probe insensitive to Mach number, angle of attack, and angle of yaw are presented in reference 10. This approach combines the idea of distributing static probe cross-sectional area with the idea of using noncircular cross sections to render probes with the desired characteristics. This type of probe, however, requires special care in cross-sectional contouring and hole location.

The purpose of the present investigation was to design and develop a probe of short length and good angle-of-attack characteristics for use in inlet, nozzle, and model flows. The primary constraints of a static-pressure probe for the proposed usage are that the probe be essentially insensitive to probe angle of attack and circumferential static hole location while having the static-pressure holes located as close to the probe tip as possible. Other desirable characteristics of the static-pressure probe design are that the measured static pressure be as close to the true static pressure as possible, and the static-pressure measurement be as insensitive to Mach number effects as possible. In an attempt to satisfy these design constraints, a static-pressure probe design has been

developed and the results of a preliminary experimental investigation are presented in reference 11. The probes of the present investigation were constructed by use of more precise methods than those of reference 11 and were experimentally calibrated at Mach numbers of 2.5 and 4.0 and for angles of attack up to 12^{o}.

SYMBOLS

A,B,C	constants
D	tube diameter
M	Mach number
p	static pressure
R_N	probe nose radius
y	distance normal to probe axis
x	axial distance from probe tip
α	angle of attack (angle between stream flow direction and probe center line)
β	cone-tip half-angle
θ	surface angle
ω	tangent cone half-angle

Subscripts:

ec	end of tangent conic curve section of probe
∞	stream conditions

NEW PROBE DESIGN

The primary desired properties of the present static-pressure probe design are that the probe be essentially insensitive to probe angle of attack and have the static-

pressure holes as close to the probe tip as possible. However, theoretical evaluation was limited to consideration of an angle of attack of 0° because no theoretical averaging method for surface pressures was immediately available from which probe readings could be determined. Therefore, the angle of attack and circumferential static hole-location (with the probe at angle of attack) effects were evaluated experimentally. The computer program used in the present theoretical evaluation is that of reference 12 and consists of a blunt-body program joined to a characteristic program. This theoretical method was used to evaluate the conventional static probe design presented in figure 1. Figure 1 also shows the static-pressure distribution along the surface of the conventional static probe design. The static holes are seen to be located approximately 10 tube diameters downstream of the cone-tube shoulder where the pressure on the surface of the probe becomes nearly equal to stream static. Note that there is a point at the shoulder of the conventional probe where the surface static pressure falls below the free-stream value, but it does so very sharply. This sharp drop can be replaced by a more gradual change, however, by replacing the sharp shoulder with a smooth fairing between the cone and the tube. Figure 2 shows the pressure distribution for two stream Mach numbers on such a fairing as a function of surface slope. The static pressure becomes equal to stream static at a surface slope around 3.5° to 4° for these Mach numbers. If the fairing is terminated at this point and joined to a tangent cone section of approximately 3° half-angle, the pressure distribution is, as shown in figure 3, where a pressure close to stream static is maintained for a finite distance along the tangent cone section.

Theoretical pressure distributions were calculated for the probe of the general design shown in figure 4, which consists of a conical tip followed by a tangent conic curve, a tangent cone section, and the cylindrical tube body. The probe tip shape used in these calculations consisted of a 20° included angle slightly blunted cone from a distance of 0 to 100 nose radii from the tip followed by a tangent conic curve section from 100 to 260 nose radii from the tip and then a tangent cone section. Three sets of theoretical calculations were made for a probe tip with a 20° included angle cone (cone-tip half-angle $\beta = 10^{\circ}$). A set of calculations were made, one each, for body shapes with tangent cone half angles ω of 2°, 3°, and 4°, and a tangent conic curve section which can be represented by a curve (in the xy-plane) of the form

$$\frac{y}{R_N} = \pm\left[A\left(\frac{x}{R_N}\right)^2 + B\,\frac{x}{R_N} + C\right]^{1/2}$$

The results of these theoretical calculations are presented in figures 5, 6, and 7 for stream Mach numbers of 2.5, 3.0, 4.0, and 5.0. Figure 5 presents theoretical surface pressures as a function of x/R_N $\left(\text{or } x/y_{ec} \text{ to be discussed later}\right)$, stream Mach number, and tangent cone half-angle ω. Figure 6 presents the theoretical surface pressures

as a function of the tangent cone half-angle ω and stream Mach number for the axial location $x/R_N = 280$. Figure 7 is a similar presentation for the axial location $x/R_N = 340$. The theoretical pressure distributions presented in figure 5 indicate that a minimum in surface pressure occurs soon after the beginning of the tangent cone section (near x/R_N of 280) and that this minimum is characterized by a region of nearly constant pressure. The theoretical results for the axial station of x/R_N of 340 was chosen because it approaches the axial limit of this calculation. Figures 6 (for $x/R_N = 280$) and 7 (for $x/R_N = 340$) both indicate that minimum stream Mach number effects occur for a tangent cone half-angle of about 1.5°. However, the point at which the surface static pressure equals the stream static pressure for these minimum Mach number effects would occur further downstream on the tangent cone surface than the $x/R_N = 340$ station. To locate the static holes so far downstream (greater than the $x/R_N = 340$ station) from the probe tip would violate one of the primary probe design constraints. Therefore, the static holes were located immediately downstream of the tangent conic curve section (that is, on the tangent cone section). Location of the holes in this nearly constant pressure region would also make the probe somewhat insensitive to effects of inaccuracies in hole location. The minimum distance at which the static holes can be located from the probe tip and still be in this minimum pressure region downstream of the end of the conic curve section is determined by the length and included angle of the conical tip. The length can be reduced only to the point that the tube diameter at the hole location is large enough to accommodate static holes of realistic size (for rapid response). The angle cannot be increased beyond the point of shock detachment for the flow Mach number.

MODELS

Based on the theoretical results given in figures 5, 6, and 7, four static-pressure probes were constructed and experimentally calibrated in the $M = 4.0$ and $M = 2.5$ blowdown nozzles. Figure 8 presents outlines of the probes calibrated; these outlines were obtained by an optical technique. Two of these probes have 10° half-angle cone tips (figs. 8(a) and 8(b)) and two have 20° half-angle cone tips (figs. 8(c) and 8(d)). One of the 10° included angle cone tips has a 2° half-angle tangent cone section (fig. 8(a)) and one tip has a 3° half-angle tangent cone section (fig. 8(b)). One of the 20° half-angle cone tips has a 2° half-angle tangent cone section (fig. 8(c)) and one tip has a 3.5° half-angle tangent cone section (fig. 8(d)). Four static holes (0.343-mm diameter) are located at 90° intervals about each 2°, 3°, or 3.5° half-angle tangent cone section. In the construction of these probes, the curved conic section was obtained by honing the intersection of the cone tip and the tangent cone into a smooth transition region. This technique resulted in there being little control on the location of the beginning and end of the curved conic section. Some probe asymmetries due to the fabrication of these probes is indicated in figure 8.

TEST PROCEDURE AND DATA REDUCTION

The experimental calibrations of static-pressure probes of the new design were conducted in a 0.2285-meter-square constant-area duct section downstream of the Mach number 4.0, blowdown nozzle at a nominal stagnation pressure of 1.517 MN/m^2. Additional experimental calibrations were conducted in a 0.0761-meter-by-0.127-meter constant-area section downstream of the Mach number 2.5 blowdown nozzle at a nominal stagnation pressure of 1.896 MN/m^2. All the calibrations were conducted over a range of angle of attack (angle between stream flow direction and probe center line) of $\pm 15^{\circ}$, the change in probe angle of attack occurring in the same plane as two of the static holes. The static probe tips were then rotated 45° so that a plane through any two opposing static holes and the probe axis were at 45° to the plane in which the probe angle of attack was changed and then the probe tip was again calibrated experimentally for $\pm 15^{\circ}$ about the chosen zero for the probe direction. The rake (rake for $M_{\infty} = 4.0$ tests is shown in fig. 9) in which the static-pressure probe tips were mounted was designed to keep the ends of the probe tips in the same spot in the tunnel during the changing of the angle of attack of the probe. The data taken during each experimental calibration test consisted of probe static pressure as a function of probe angle of attack and tunnel stagnation pressure. During a separate test, tunnel pitot pressures were taken in the same spot in the tunnel where the end of the static probe tip was located. Tunnel static, pitot, and stagnation pressures were measured by use of 0.0345 MN/m^2 absolute ($M_{\infty} = 4.0$ static pressure), 0.345 MN/m^2 absolute ($M_{\infty} = 4.0$ pitot pressure), 3.45 MN/m^2 absolute ($M_{\infty} = 2.5$, 4.0 stagnation pressure), 0.172 MN/m^2 absolute ($M_{\infty} = 2.5$ static pressure), and 1.04 MN/m^2 absolute ($M_{\infty} = 2.5$ pitot pressure) pressure transducers and were recorded on an 18-channel visual recorder along with probe angle of attack. The tunnel pitot pressure is used in conjunction with the measured tunnel stagnation pressure to determine a stream static pressure. In the data reduction the static pressure measured by use of the static probe tips of the new design and the stream static pressure determined from the tunnel pitot-pressure measurements were nondimensionalized by dividing by their respective tunnel total pressure to eliminate tunnel total-pressure differences between test runs. For the $M_{\infty} = 4.0$ calibration tests, it was found that the 0° position of the probe mechanism and the tunnel flow were misalined by approximately 3.6° and the data were adjusted accordingly. Experimental results presented in this paper for the $M_{\infty} = 4.0$ calibration tests are for an angle of attack of $\pm 1.4^{\circ}$ and for the $M_{\infty} = 2.5$ calibration, tests are for an angle of attack of $\pm 2.5^{\circ}$.

RESULTS AND DISCUSSION

In the comparison of experimental and theoretically predicted local flow parameters on a blunt-nosed axisymmetric body such as the conical-tip static probe, the nose radius

or diameter is usually used as a normalizing parameter when the region of the body being considered is close (less than about 50 nose radii) to the tip of the body. (See ref. 13.) When the region of interest on a blunted conical body is greater than about 50 nose radii from the cone tip, the nose radius is no longer pertinent for this purpose and the normalizing parameter then involves the cone angle and the axial distance from the cone tip. Based on these factors, the parameter chosen to nondimensionalize the geometric shape of the experimental probes as well as the body shapes used in the theoretical calculation is the radius of the probe at the end of the curved conic section y_{ec}.

The geometric contours of the four probes experimentally calibrated were nondimensionalized by the radius of the probes at the end of their respective curved conic sections and the results are presented in figures 10 and 11. The nondimensionalized body shape for the probe with $\beta = 10^{\circ}$ followed by a curved conic section and then a $\omega = 2^{\circ}$ tangent conic section is presented in figure 10(a). Also shown in figure 10(a) is the theoretical body shape used in the corresponding theoretical calculations along with the predicted static-pressure distribution on the body surface for $M_{\infty} = 4.0$ and $M_{\infty} = 2.5$. Similar curves for the probe with a $\beta = 10^{\circ}$ conical tip and a $\omega = 3^{\circ}$ tangent cone are presented in figure 10(b). The nondimensionalized body shapes for the two $\beta = 20^{\circ}$ conical tipped probes (followed by a curved conic section), one with a $\omega = 2^{\circ}$ tangent cone section and one with a $\omega = 3.5^{\circ}$ tangent cone section, are presented in figure 11. The theoretical body shape for a $\beta = 20^{\circ}$ initial conical tip (followed by a curved conic section) and a $\omega = 3^{\circ}$ tangent cone section is also presented in figure 11 along with the predicted static-pressure distribution for $M_{\infty} = 4.0$ and $M_{\infty} = 2.5$. All theoretical calculations are for an angle of attack of 0°. The axial location of the respective static-pressure holes on the four probe geometries experimentally calibrated is also shown in figures 10 and 11. The favorable comparisons of surface angles in the region of the static holes with the surface angles of the sample probes calibrated reveal that construction of the present static probe is no problem.

Experimental measurements of static pressure by use of the sample probes are expressed as ratios to stream static pressure and are presented in figures 12 and 13 as a function of the tangent cone half-angle of the probe ω. The corresponding theoretical predictions of probe surface static pressure (for theoretical probe shape) are also presented. Both the experimental and theoretical results are presented in figures 12 and 13 and are for an angle of attack of 0°. The results presented in figures 12(a) and 12(b) are for the $\beta = 10^{\circ}$ probes at stream Mach numbers of 2.5 and 4.0. The experimental and theoretical results presented in figures 13(a) and 13(b) are for the $\beta = 20^{\circ}$ probes at stream Mach numbers of 2.5 and 4.0, respectively. The spread of the experimental results in figures 12 and 13 is typical of the inaccuracy that results during the reading of the pressure trace of the visual recorder. Also plotted in figures 12(a) and 12(b) are curves representing the theoretical predictions for the static pressure at the probe static

hole locations given in figures 10(a) and 10(b). For the $\beta = 20^{\circ}$ probe tip, only one theoretical calculation was made and that was for a probe with a $\omega = 3^{\circ}$ tangent cone. The spread of the theoretical results shown in figures 13(a) and 13(b) for the $\beta = 20^{\circ}$ probe tip and a $\omega = 3^{\circ}$ tangent cone is a result of reading the predicted static pressure from the theoretical curves of figure 11 at the two probe static hole locations shown in the figure. From the results presented in figures 12 and 13, it is concluded that for an angle of attack of 0°, reasonable comparisons of theoretical predictions and experimental measurements of probe static pressure can be obtained.

The static pressures measured at angle of attack and nondimensionalized by the stream static pressure are presented in figure 14 for probes with $\beta = 10^{\circ}$ and in figure 15 for probes with $\beta = 20^{\circ}$. The calibration data of figures 14 and 15 for the static holes rotated 45° show no consistent effects of circumferential static hole location relative to the angle of attack plane and indicate a decrease in pressure measurement with probe angle of attack. Preliminary probe calibrations (not presented) also showed no consistent effects of circumferential static hole location for other hole angles. The differences between data for positive and negative angles of attack are not understood. If an arithmetic mean value of the highest and lowest experimental (within an angle of attack of $\pm 10^{\circ}$) values of the ratio of p/p_{∞} is used as the calibration value for each probe, the true static pressure for $M_{\infty} = 4.0$ (figs. 14(c), 14(d), 15(c), and 15(d)) could be determined within about ± 4 percent of the correct value for a range of angles of attack of $\pm 10^{\circ}$. If a similar average is used for the calibration value of p/p_{∞} for $M_{\infty} = 2.5$ (figs. 14(a), 14(b), 15(a), and 15(b)), the true static pressure could be determined within about ± 2 percent over the same angle-of-attack range. Therefore, comparison of the angle-of-attack calibration data for $M_{\infty} = 4.0$ with that for $M_{\infty} = 2.5$ indicates that the angle of attack effects decrease with decreasing Mach number. If, however, the probe angle of attack is restricted to within $\pm 7^{\circ}$, the true stream static pressure could be determined to within about ± 2 percent.

CONCLUSIONS

A static-pressure probe design concept has been developed which has the static holes located close to the probe tip and is relatively insensitive to probe angle of attack and circumferential static hole location. Probes were constructed with 10° and 20° half-angle cone tips followed by a tangent conic curve section and a tangent cone section of 2°, 3°, or 3.5° and were tested at Mach numbers of 2.5 and 4.0 and angles of attack up to 12°. From the results of the tests, the following conclusions were obtained:

1. The construction of the probes was not difficult with standard shop techniques.

2. For stream Mach numbers of 2.5 and 4.0 and probe angle of attack (angle between stream flow direction and probe center line) within $\pm 10^{\circ}$, values of stream static pressure can be determined from the probe calibration to within about ± 4 percent.

3. If the probe is alined within about 7° of the flow, the stream static pressures can be determined to within 2 percent from the probe calibration.

4. For an angle of attack of 0°, good comparisons are obtained between theoretical predictions of probe static-pressure and experimental probe calibrations.

5. Theoretical predictions indicate that a probe of the present design with a 10° cone half-angle tip and a 1.5° half-angle tangent cone would be the least sensitive to Mach number.

Langley Research Center,
National Aeronautics and Space Administration,
Hampton, Va., May 1, 1975.

REFERENCES

1. Holder, D. W.; North, R. J.; and Chinneck, A.: Experiments With Static Tubes in a Supersonic Airstream – Parts I and II. R. & M. No. 2782, British A.R.C., July 1950.

2. Wilson, L. N.: An Experimental Investigation of Reynolds Number Effects on Supersonic Static Probes. Tech. Note No. 3, Inst. Aerophys., Univ. of Toronto, Sept. 1954.

3. Lindsey, J. L.: Interference Effects Due to Relative Proximity of Static-Pressure Probes in Supersonic Flow. DRL-395, Univ. of Texas (Austin), June 1957.

4. Hess, John L.; Smith, A. M. O.; and Rivell, Thomas L.: Analytic Design of Improved Static Pressure Sending Probes for All Mach Numbers. Rep. No. LB 31589 (Contract NOw 62-0297-t), Douglas Aircraft Co., Inc., Feb. 14, 1964.

5. Gracey, William: Measurement of Static Pressure on Aircraft. NACA Rep. 1364, 1958. (Supersedes NACA TN 4184.)

6. Richie, Virgil S.: Several Methods for Aerodynamic Reduction of Static-Pressure Sensing Errors for Aircraft at Subsonic, Near-Sonic, and Low Supersonic Speeds. NASA TR R-18, 1959.

7. Clippinger, R. F.; Giese, J. H.; and Carter, W. C.: Tables of Supersonic Flows About Cone-Clinders. Part I: Surface Data. Rep. No. 729, Ballistic Res. Labs., Aberdeen Proving Grounds, July 1950.

8. Hall, I. M.; Rogers, E. W. E.; and Davis, B. M.: Experiments With Inclined Blunt-Nosed Bodies at $M_0 = 2.45$. R. & M. No. 3128, British A.R.C., 1959.

9. Donaldson, I. S.; and Richardson, D. J.: Short Static Probe With Good Incidence Characteristics at Supersonic Speed. C.P. No. 1099, British A.R.C., 1970.

10. Smith, A. M. O.; and Bauer, A. B.: Static-Pressure Probes That Are Theoretically Insensitive to Pitch, Yaw and Mach Number. J. Fluid Mech., vol. 44, pt. 3, 1970, pp. 513-528.

11. Pinckney, S. Z.: An Improved Static Probe Design. AIAA J., vol. 12, no. 4, Apr. 1974, pp. 562-564.

12. Chu, C. W.; and Powers, S. A.: The Calculation of Three-Dimensional Supersonic Flows Around Spherically-Capped Smooth Bodies and Wings. AFFDL-TR-72-91, Vols. I and II, U.S. Air Force, Sept. 1972.
    Vol. I.- Theory and Applications.
    Vol. II.- Manual for Computer Programs.

13. Cubbage, James M.: Effect of Nose Bluntness and Controlled Roughness on the Flow on Two Hypersonic Inlet Center Bodies Without Cowling at Mach 5.98. NASA TN D-2900, 1965.

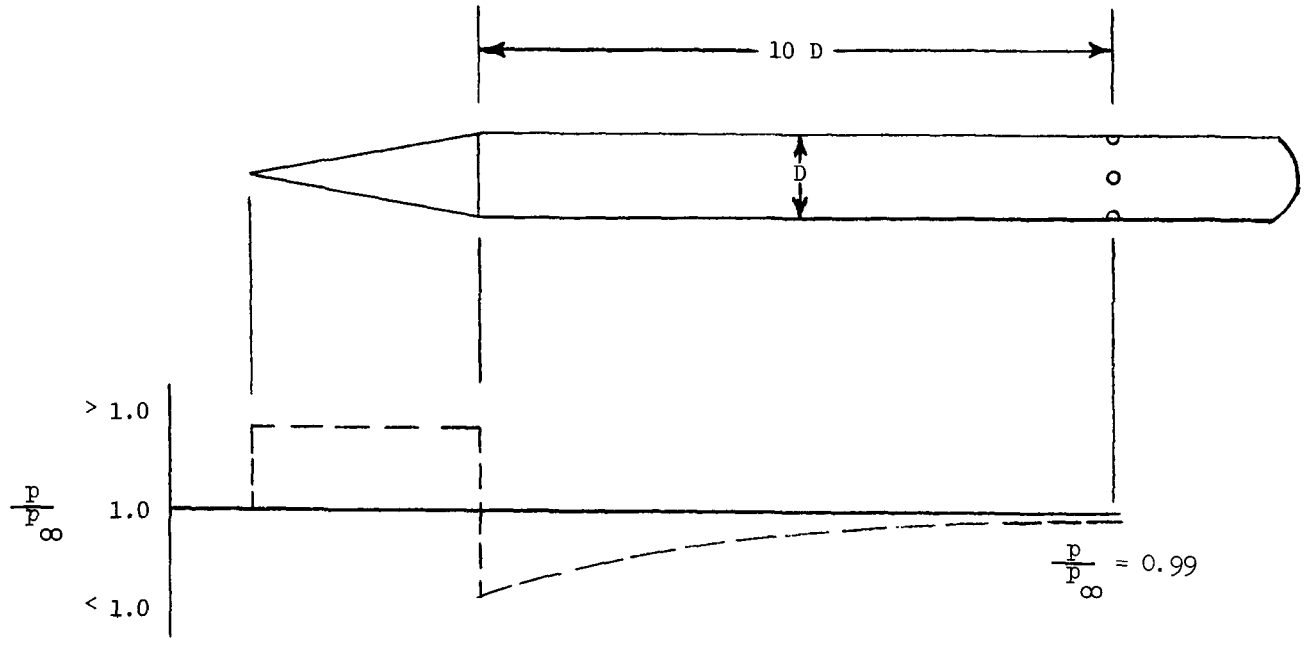

Figure 1.- Conventional static-pressure probe design and surface-pressure distribution.

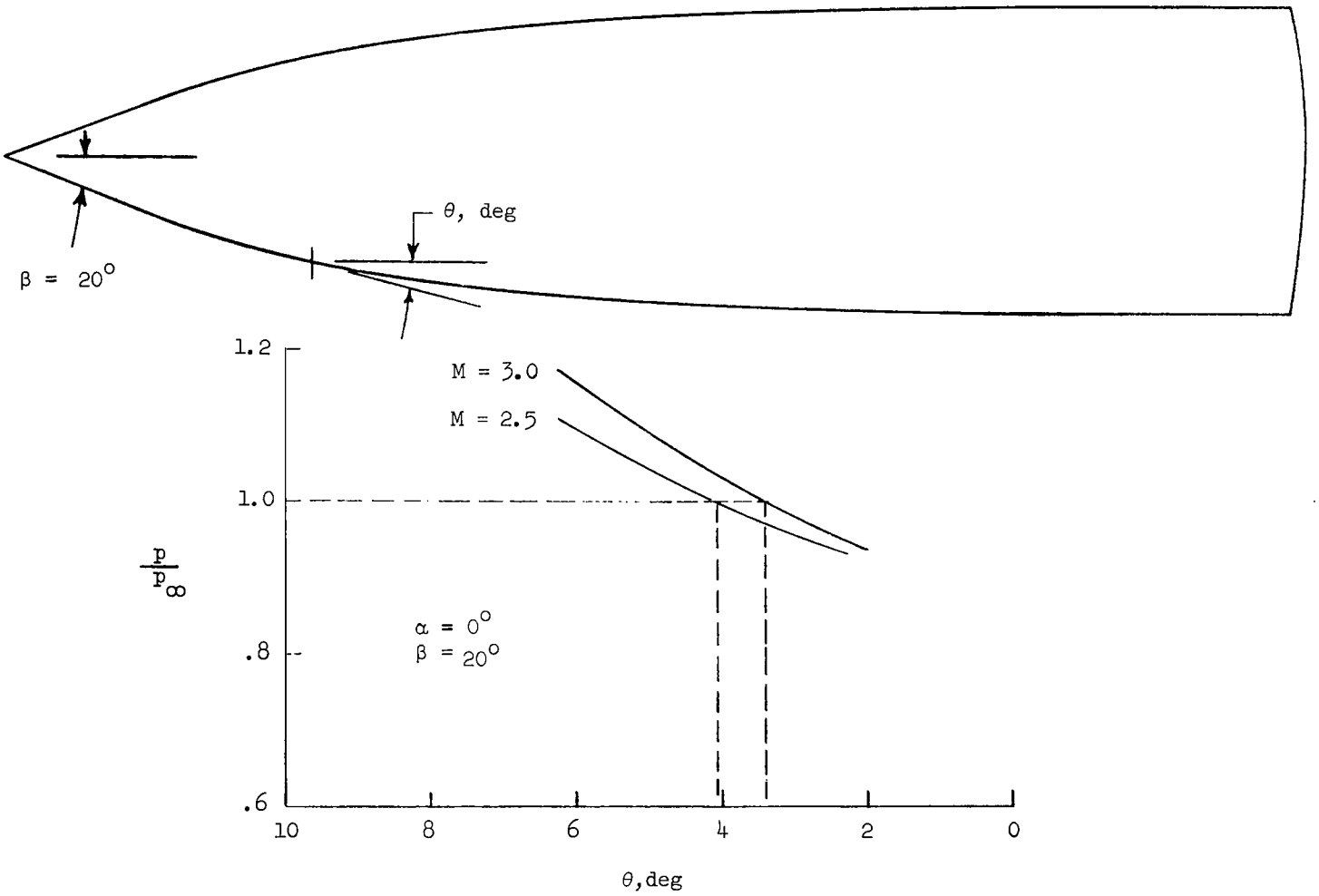

Figure 2.- Theoretically predicted pressure along the surface of a smooth fairing between the cone nose and the cylindrical afterbody.

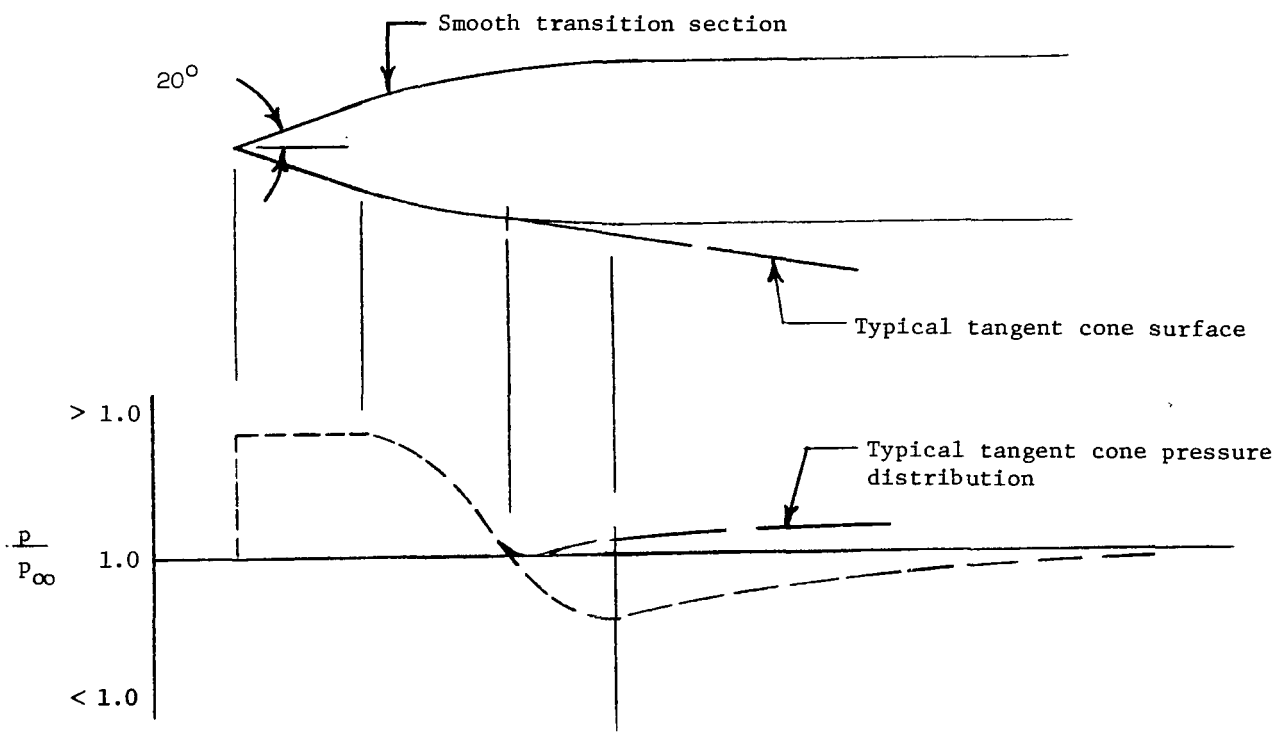

Figure 3.- Body shape which has a smooth fairing between the conical nose and cylindrical section or tangent cone surface along with typical surface-pressure distributions.

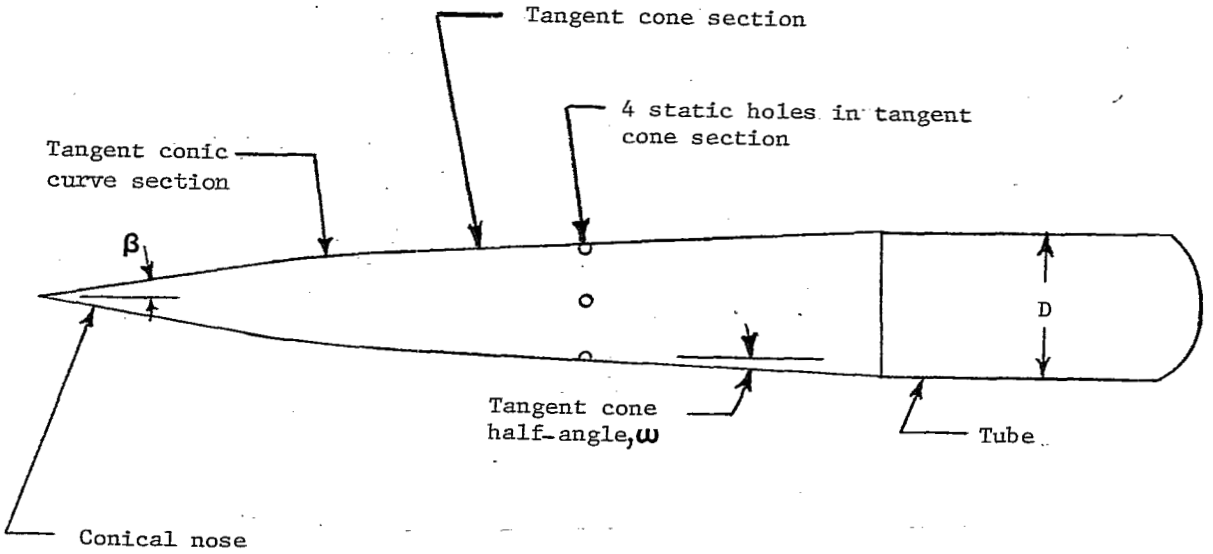

Figure 4.- Present static-pressure probe design.

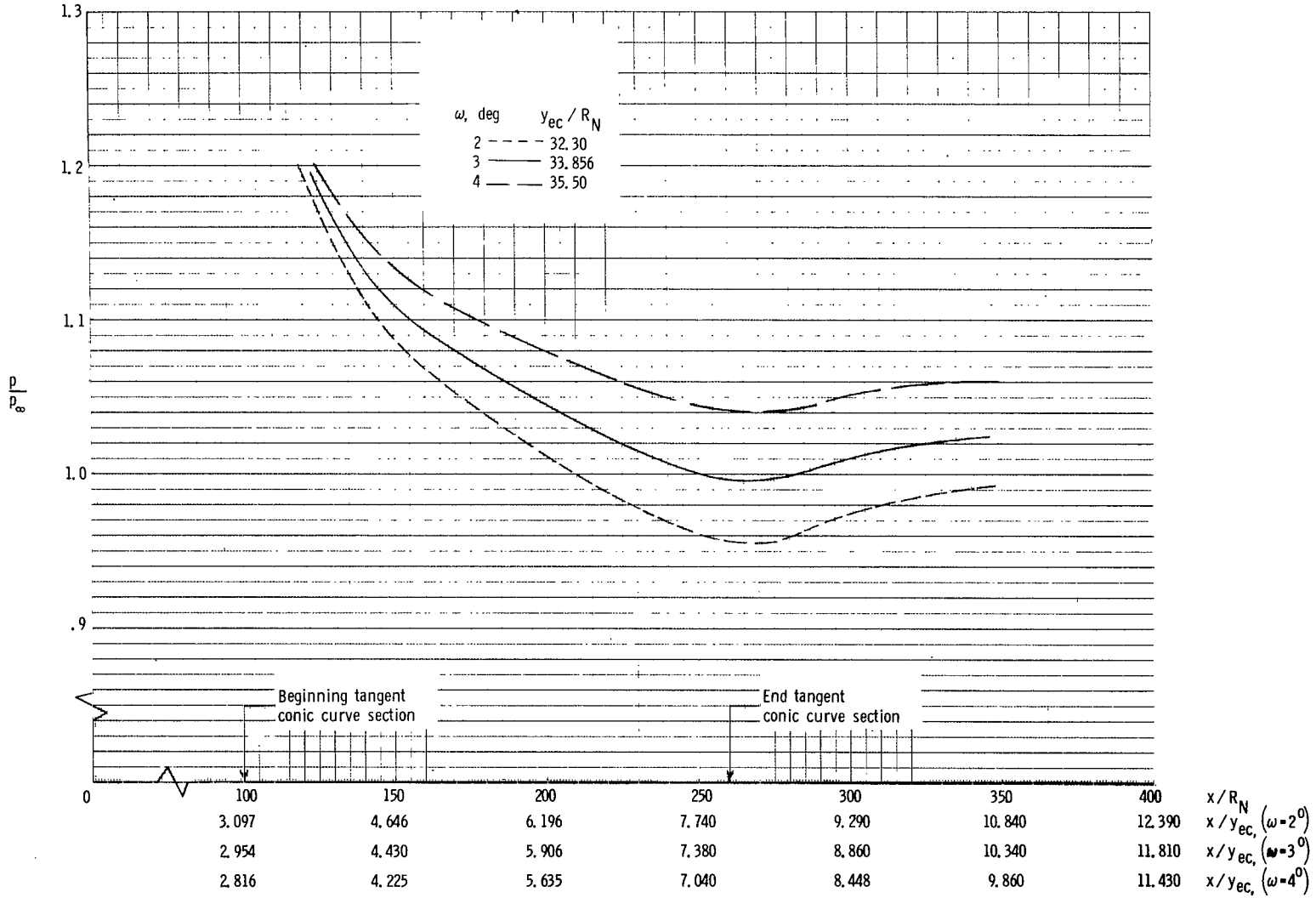

(a) $M_\infty = 2.5$.

Figure 5.- Theoretical static pressure distribution on the surface of the present static pressure probe design. $\beta = 10^\circ$.

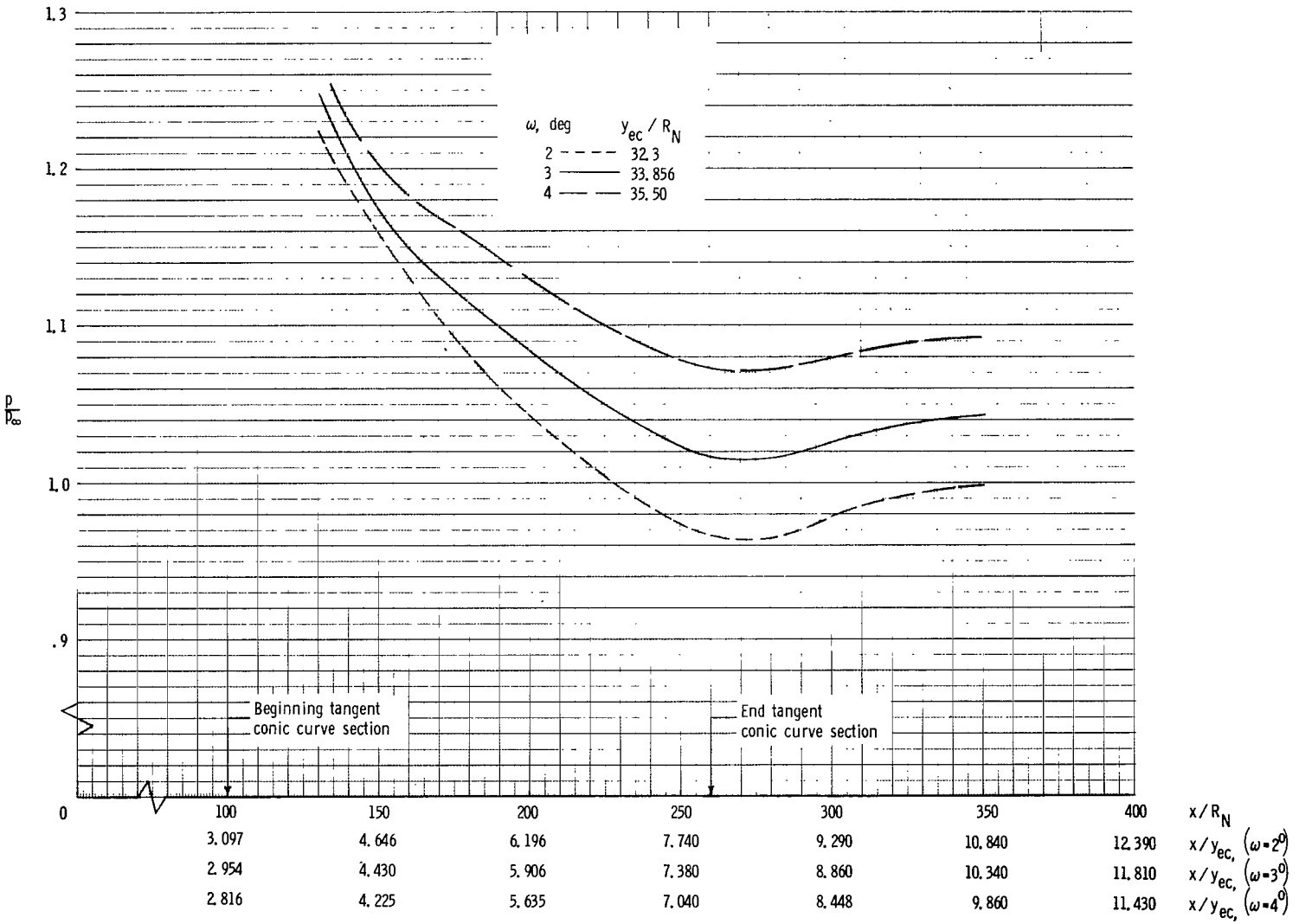

(b) $M_\infty = 3.0$.

Figure 5.- Continued.

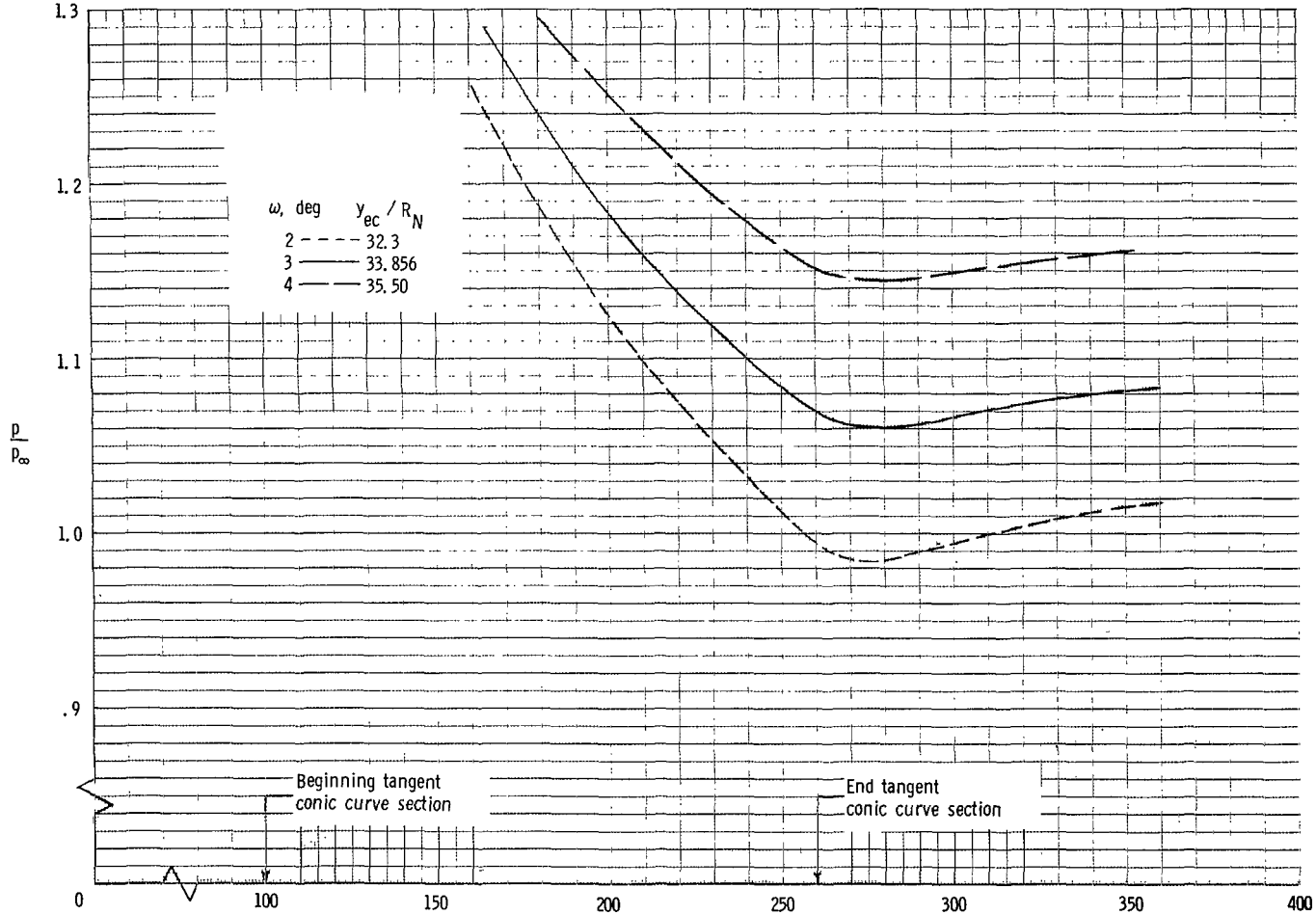

x/R_N	100	150	200	250	300	350	400
x/y_ec, (ω=2°)	3.097	4.646	6.196	7.740	9.290	10.840	12.390
x/y_ec, (ω=3°)	2.954	4.430	5.906	7.380	8.860	10.340	11.810
x/y_ec, (ω=4°)	2.816	4.225	5.635	7.040	8.448	9.860	11.430

(c) $M_\infty = 4.0$.

Figure 5.- Continued.

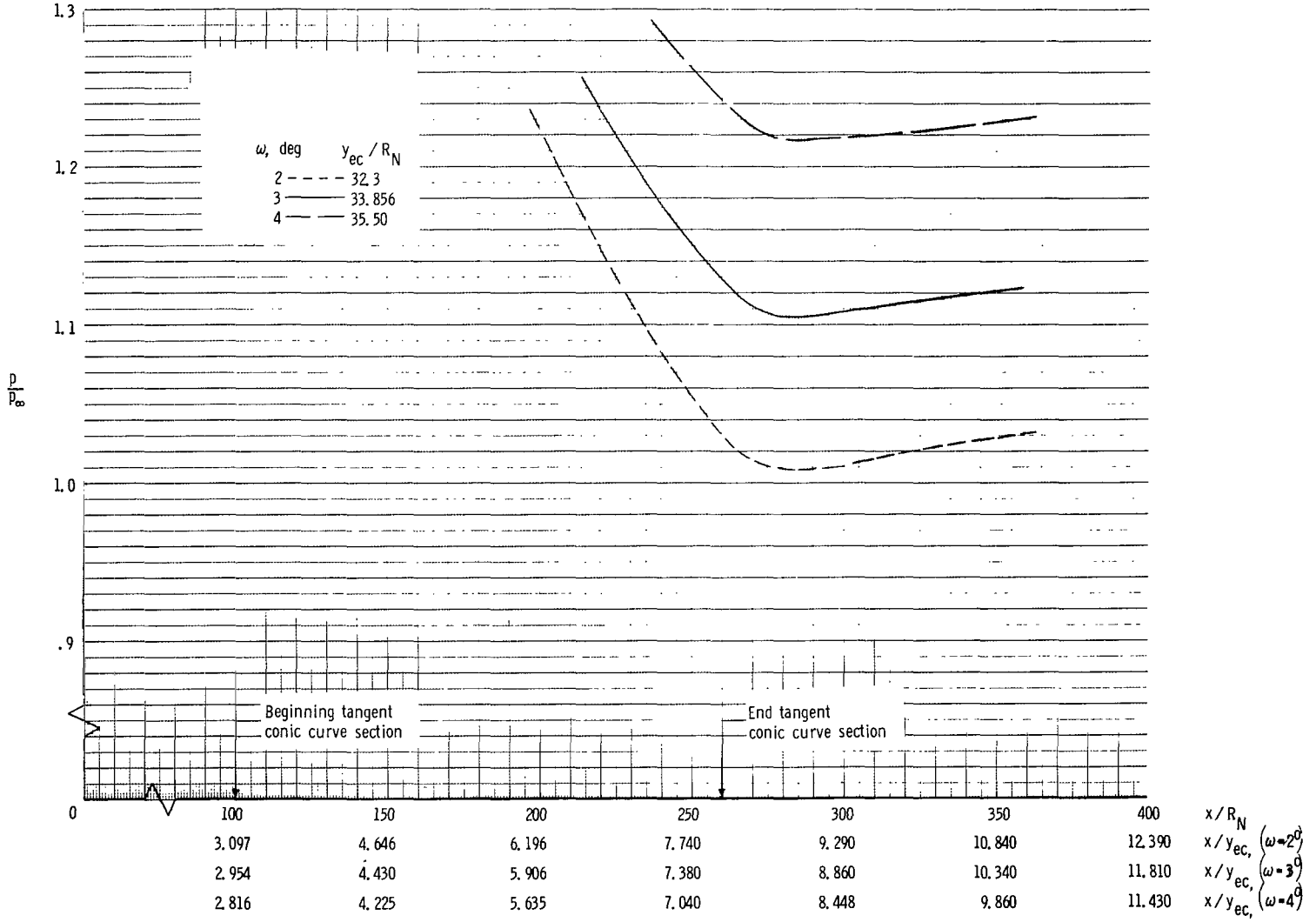

(d) $M_\infty = 5.0$.

Figure 5.- Concluded.

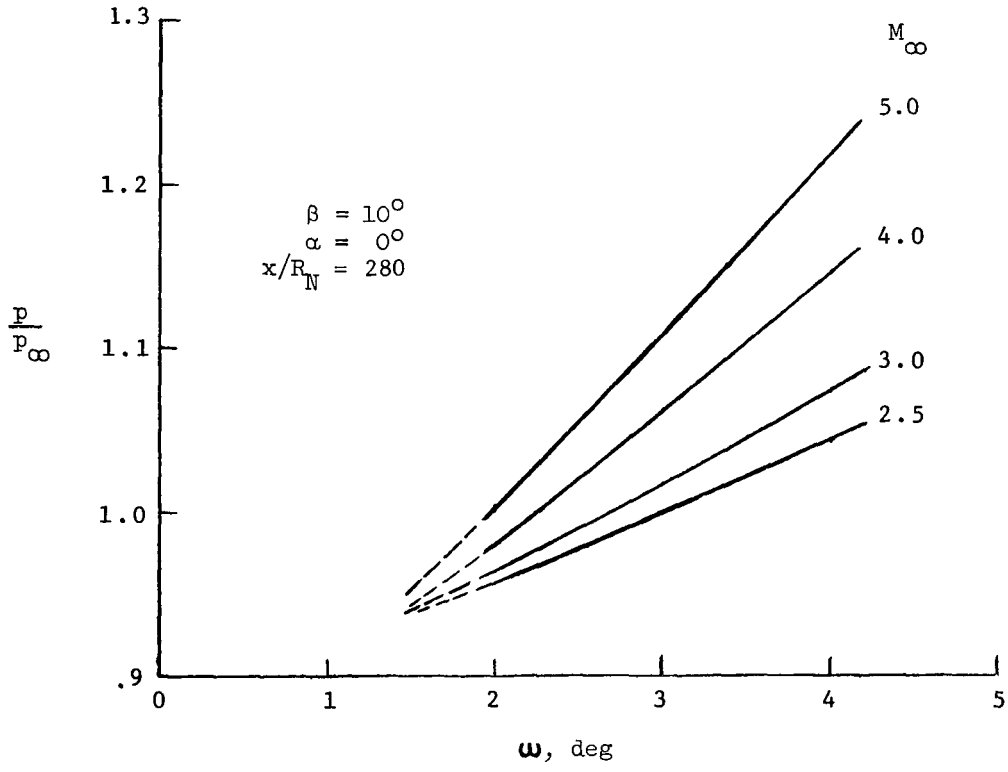

Figure 6.- Theoretical surface static pressure on the present static-pressure probe design. $x/R_N = 280$.

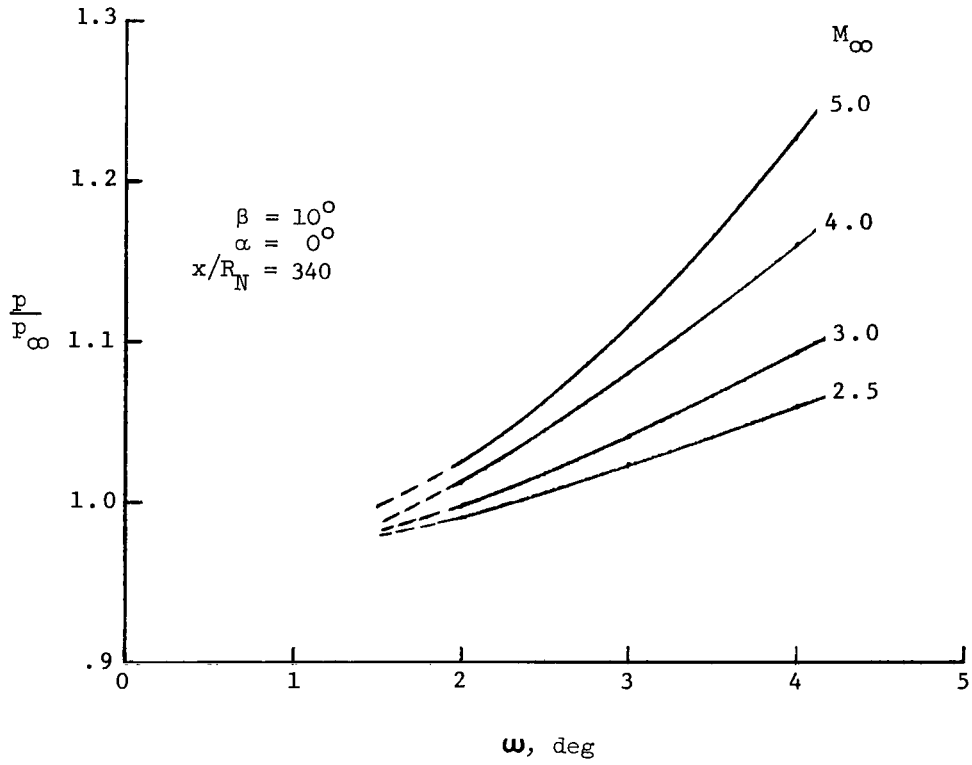

Figure 7.- Theoretical surface static pressure on the present static-pressure probe design. $x/R_N = 340$.

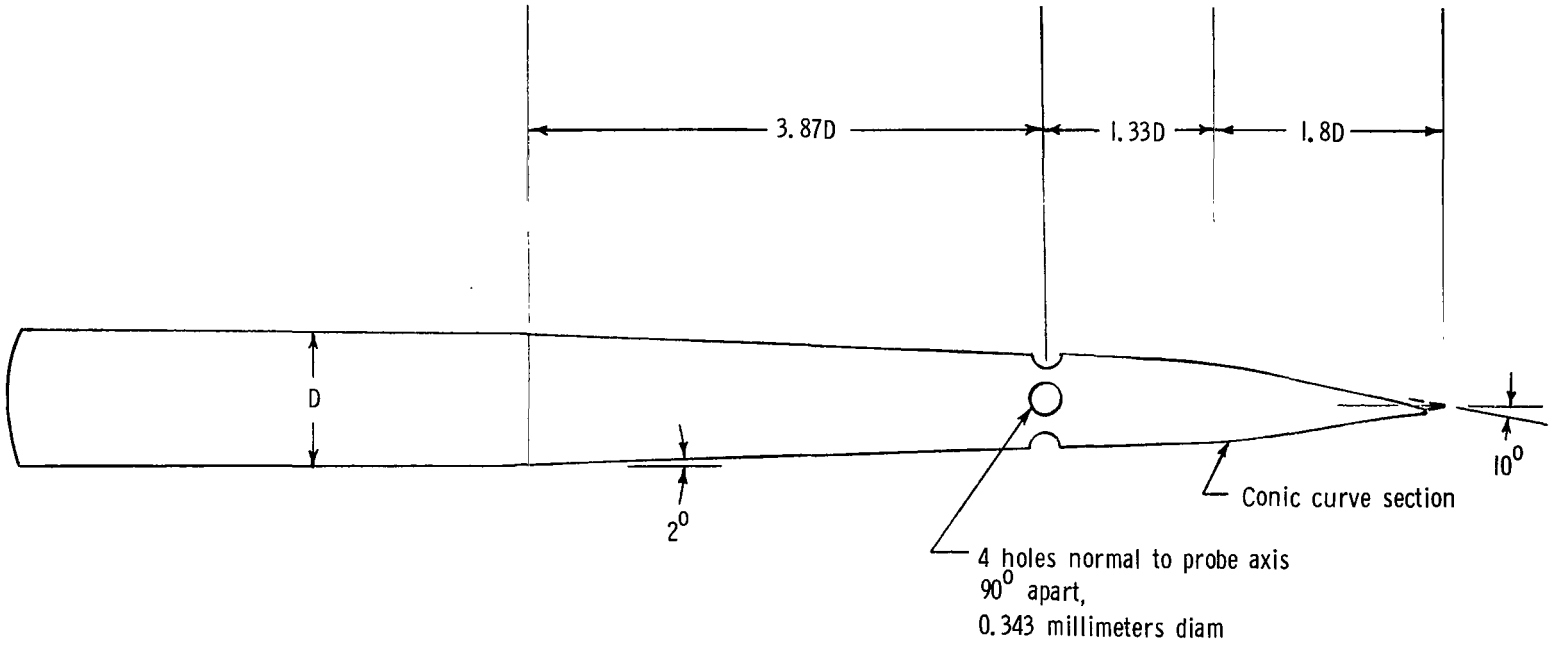

(a) $\beta = 10^{\circ}$; $\omega = 2^{\circ}$.

Figure 8.- Geometry of probes calibrated. D = 1.53 mm.

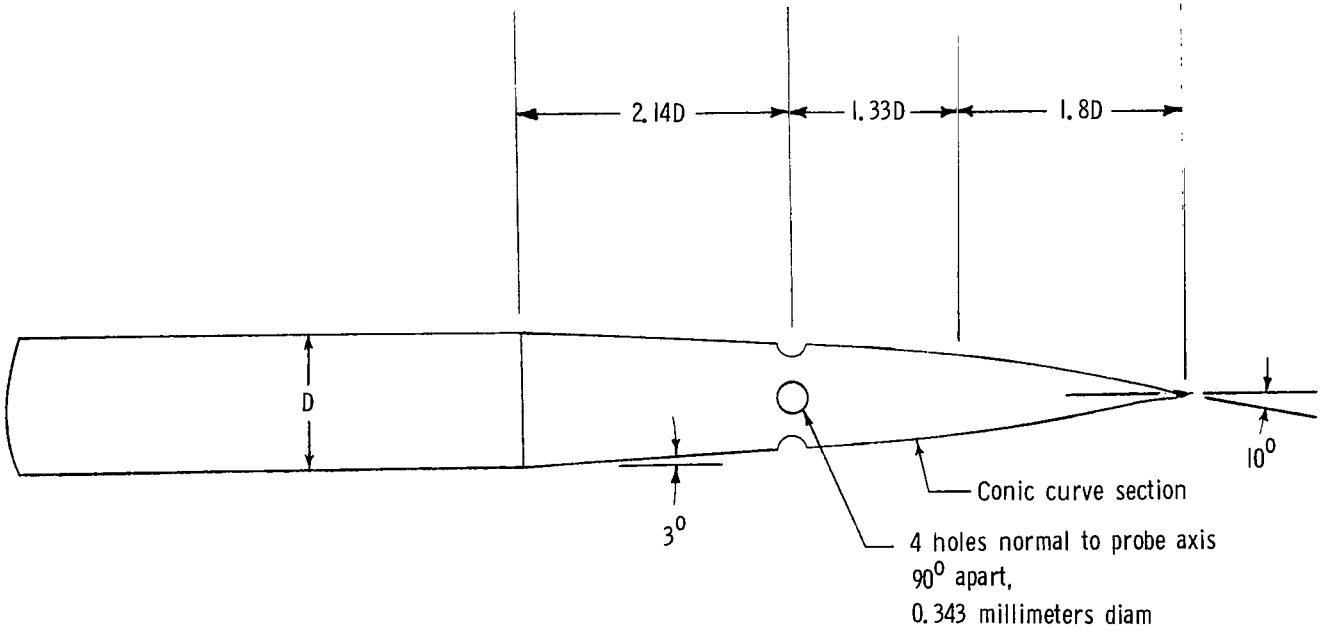

(b) $\beta = 10^{\circ}$; $\omega = 3^{\circ}$.

Figure 8.- Continued.

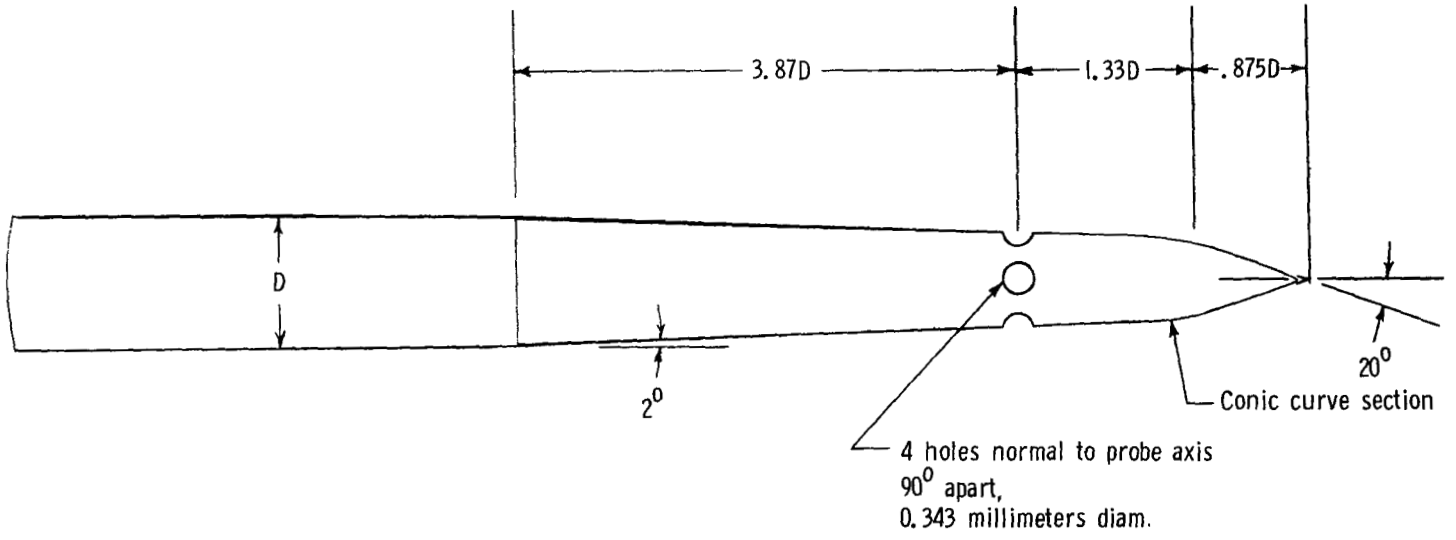

(c) $\beta = 20^{\circ}$; $\omega = 2^{\circ}$.

Figure 8.- Continued.

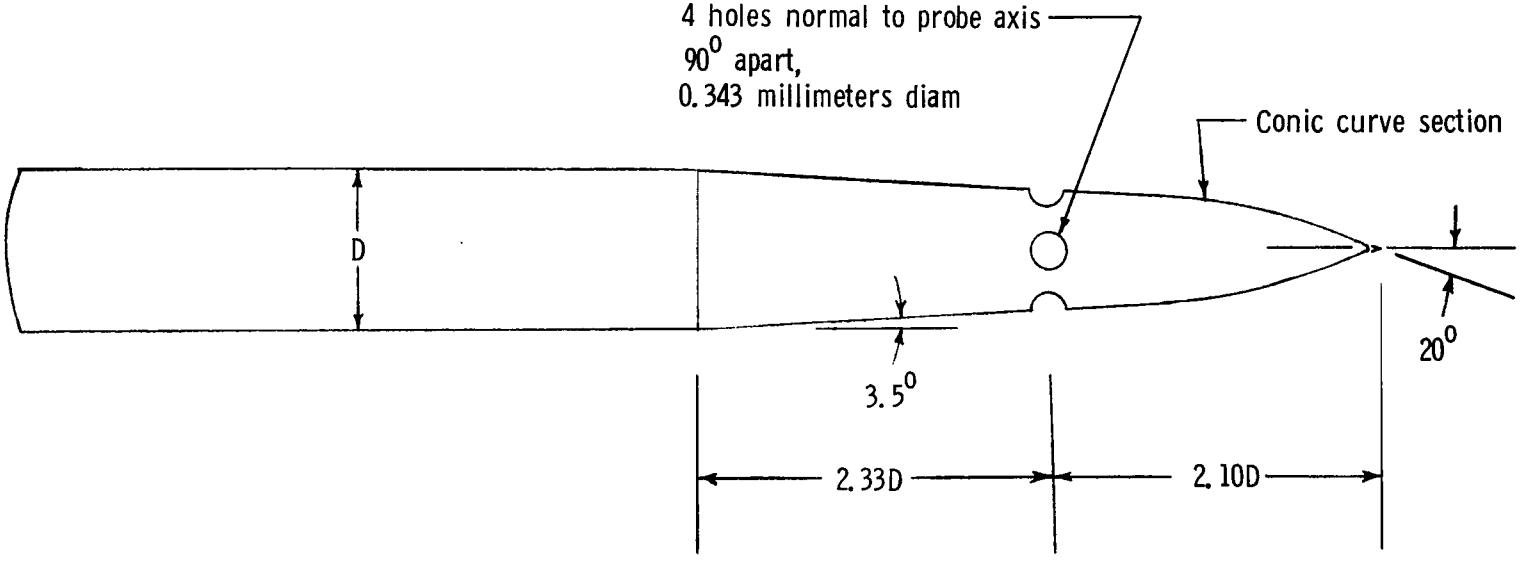

(d) $\beta = 20^{\circ}$; $\omega = 3.5^{\circ}$.

Figure 8.- Concluded.

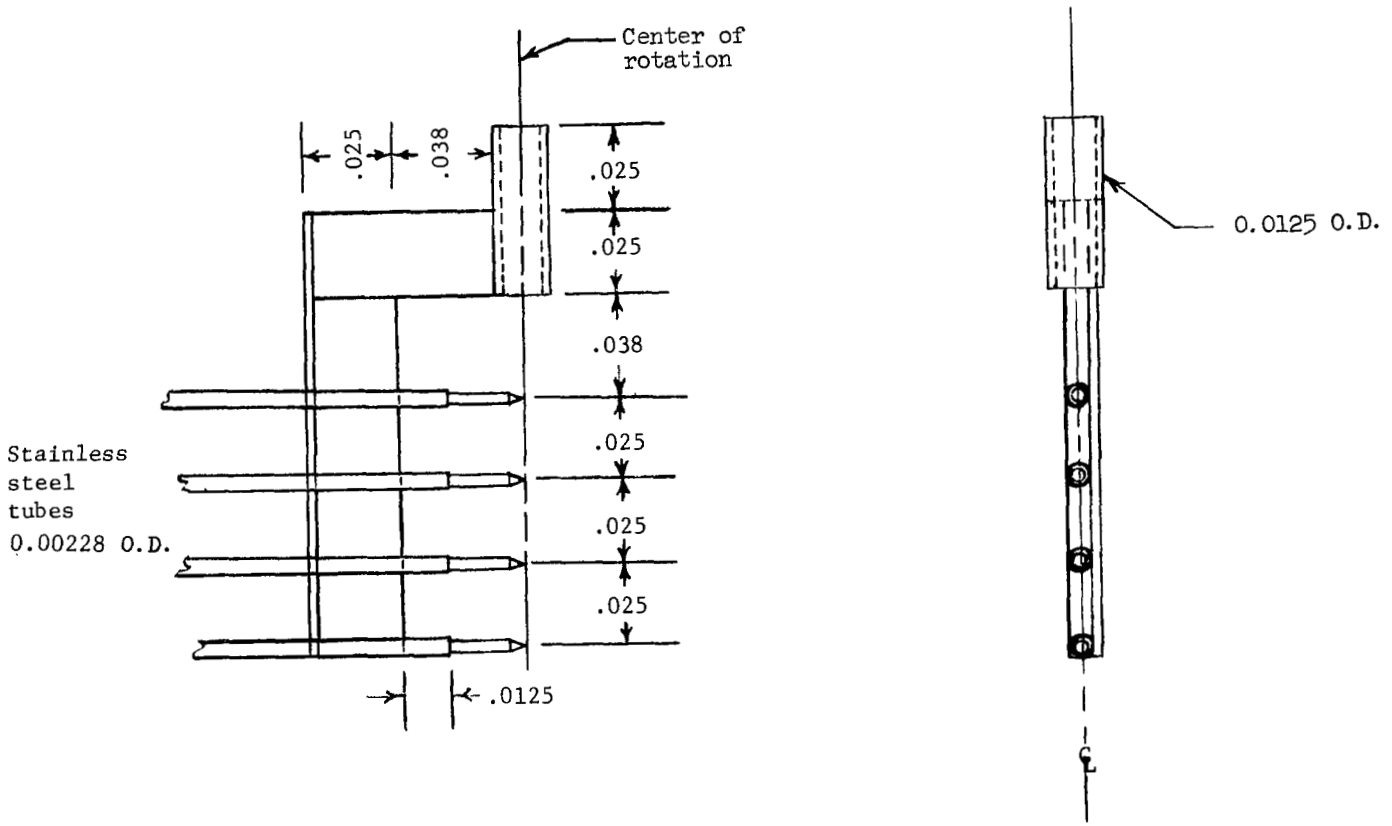

Figure 9.- Calibration rake. All dimensions are in meters.

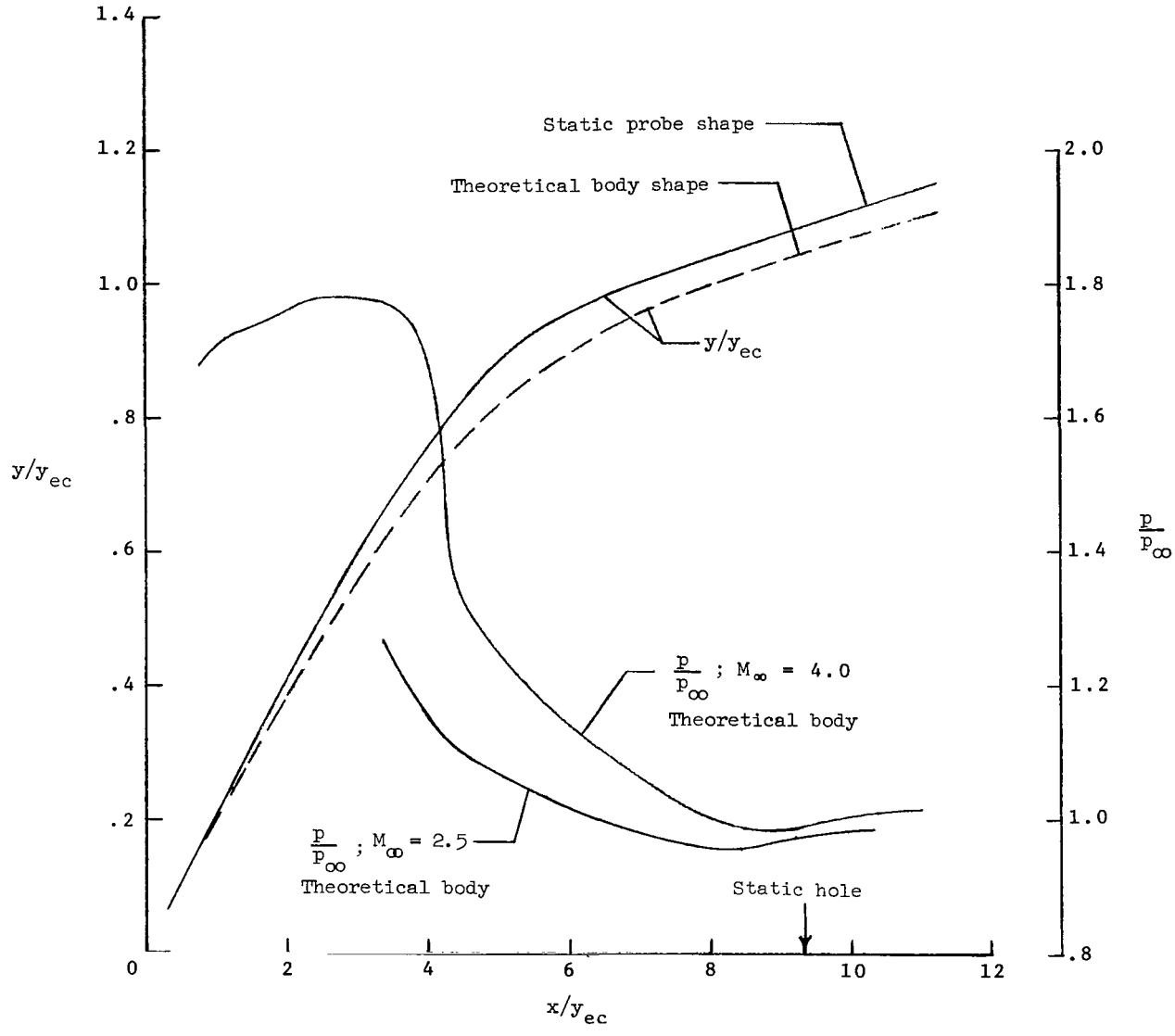

(a) $\omega = 2^o$.

Figure 10.- Theoretical surface static-pressure distributions and comparison of actual shape of probes with theoretical body shape. $\beta = 10^o$; $\alpha = 0^o$.

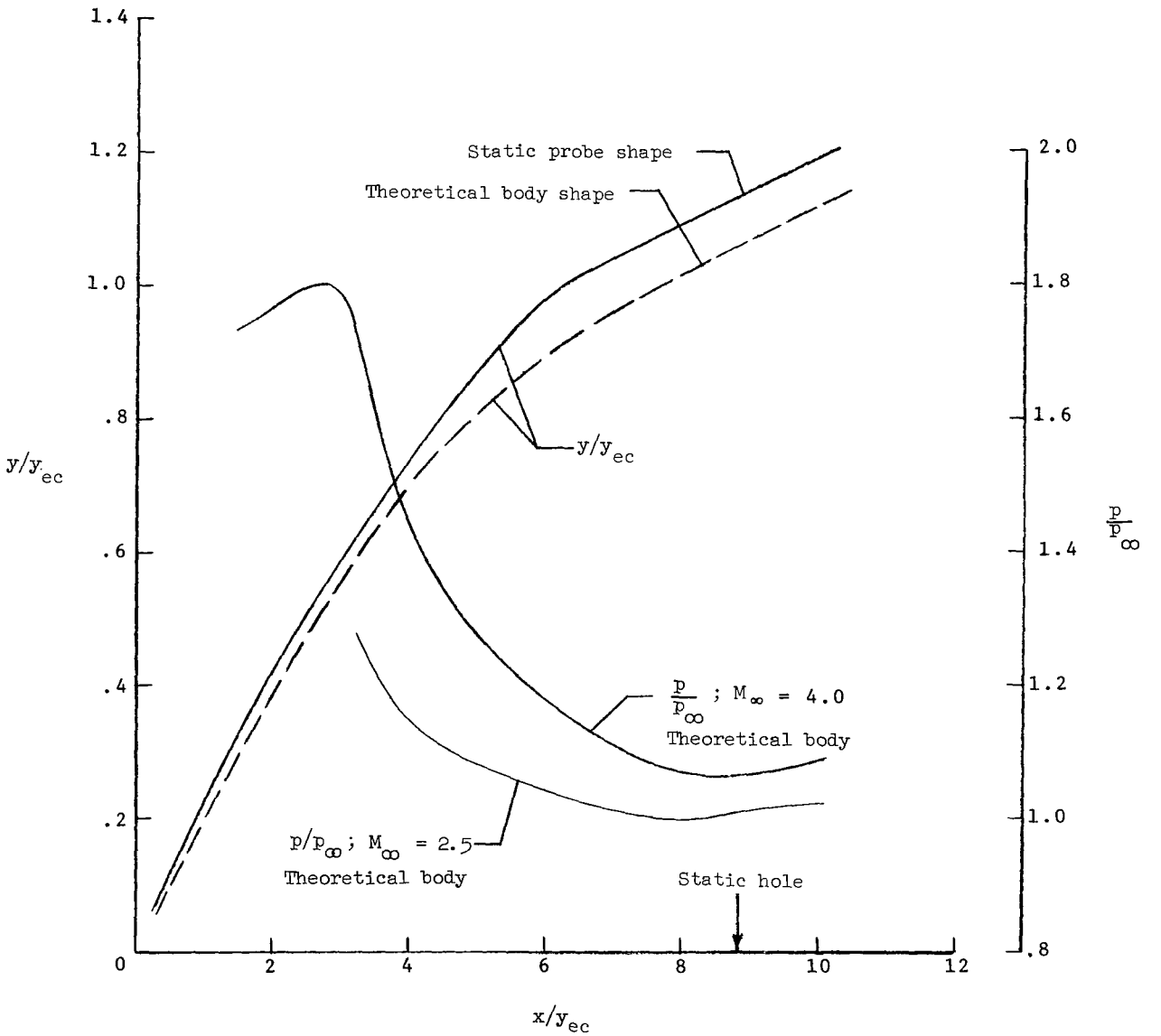

(b) $\omega = 3^{o}$.

Figure 10.- Concluded.

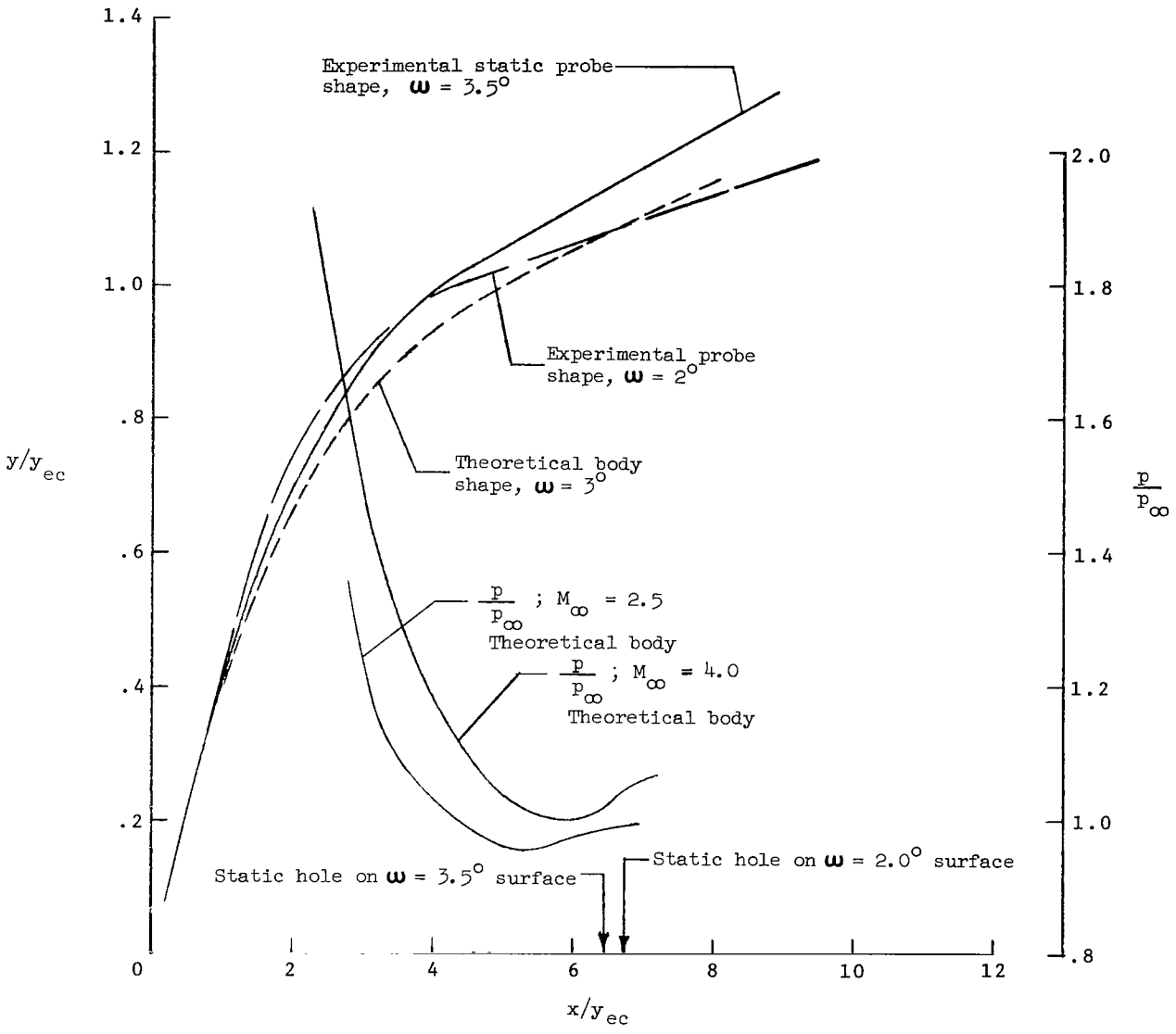

Figure 11.- Theoretical surface static-pressure distributions and comparison of actual shape of probe with theoretical body shape. $\beta = 20^{\circ}$; $\alpha = 0^{\circ}$.

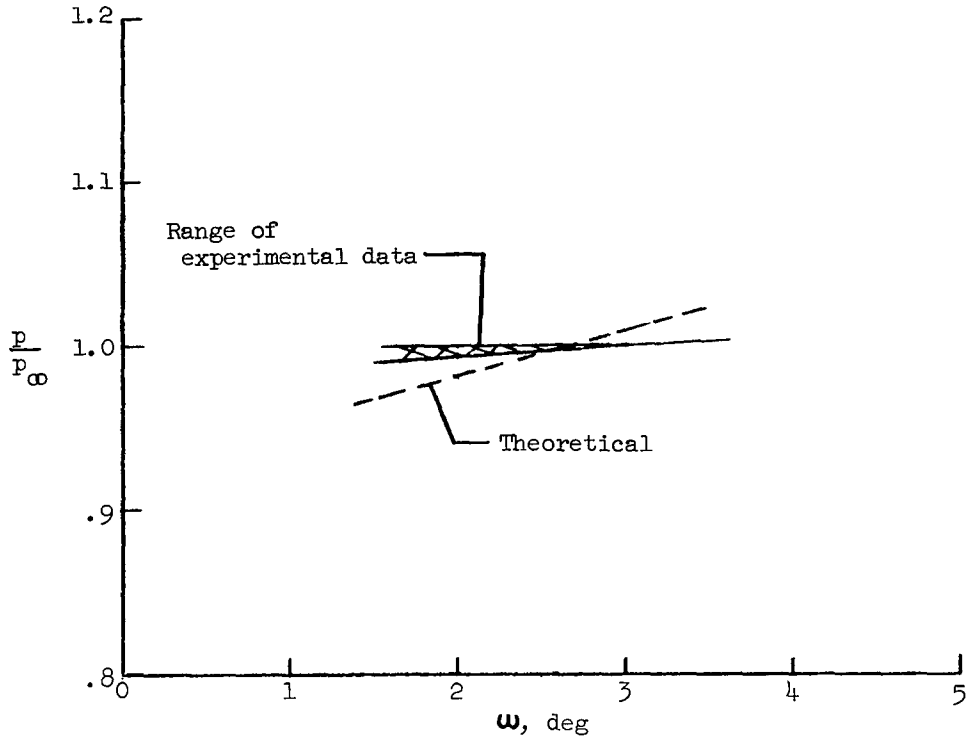

(a) $M_\infty = 2.5$.

Figure 12.- Comparison of experimental and theoretical static pressures for the present probes. $\beta = 10^o$; $\alpha = 0^o$.

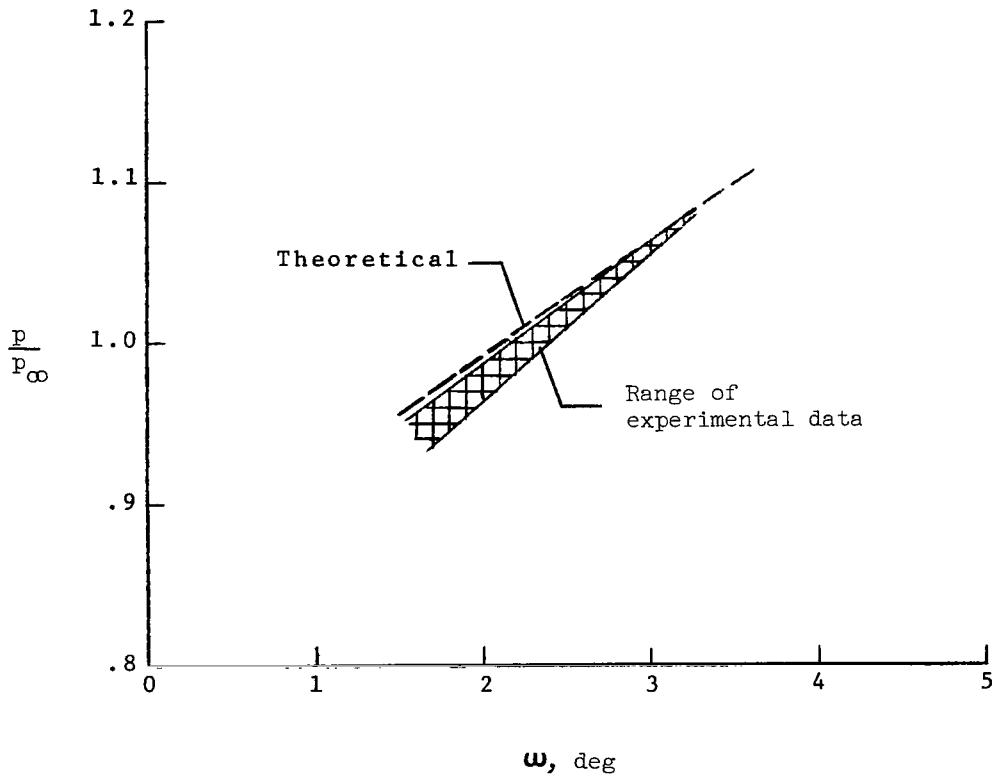

(b) $M_\infty = 4.0$.

Figure 12.- Concluded.

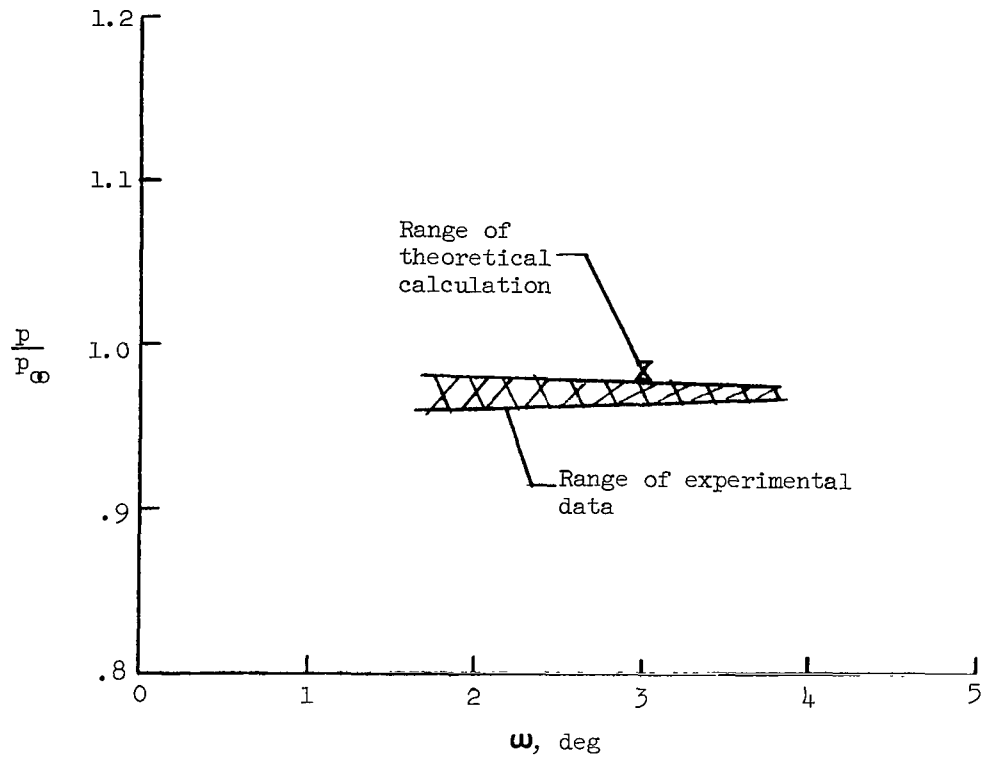

(a) $M_\infty = 2.5$.

Figure 13.- Comparison of experimental and theoretical static pressures for the present probes. $\beta = 20^o$; $\alpha = 0^o$.

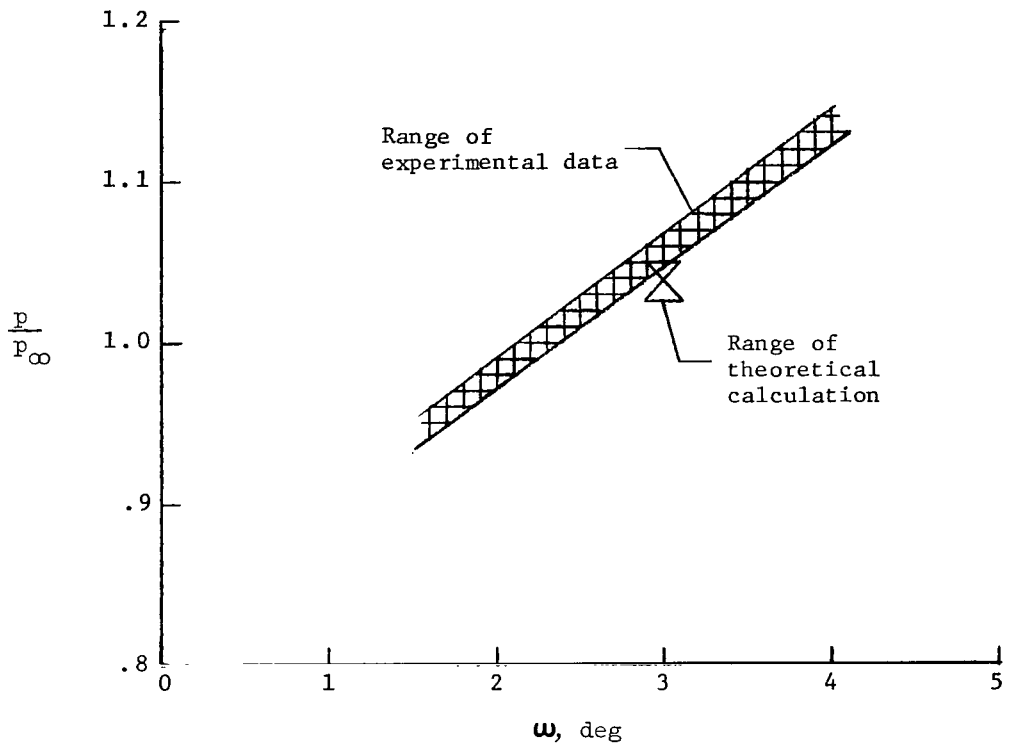

(b) $M_\infty = 4.0$.

Figure 13.- Concluded.

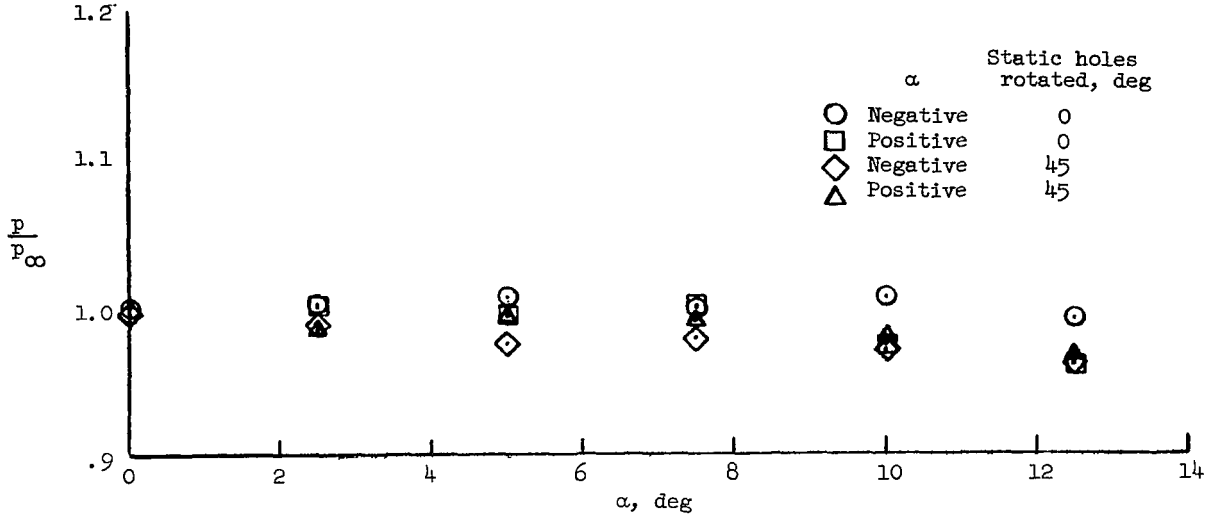

(a) $\omega = 2^{o}$; $M_{\infty} = 2.5$.

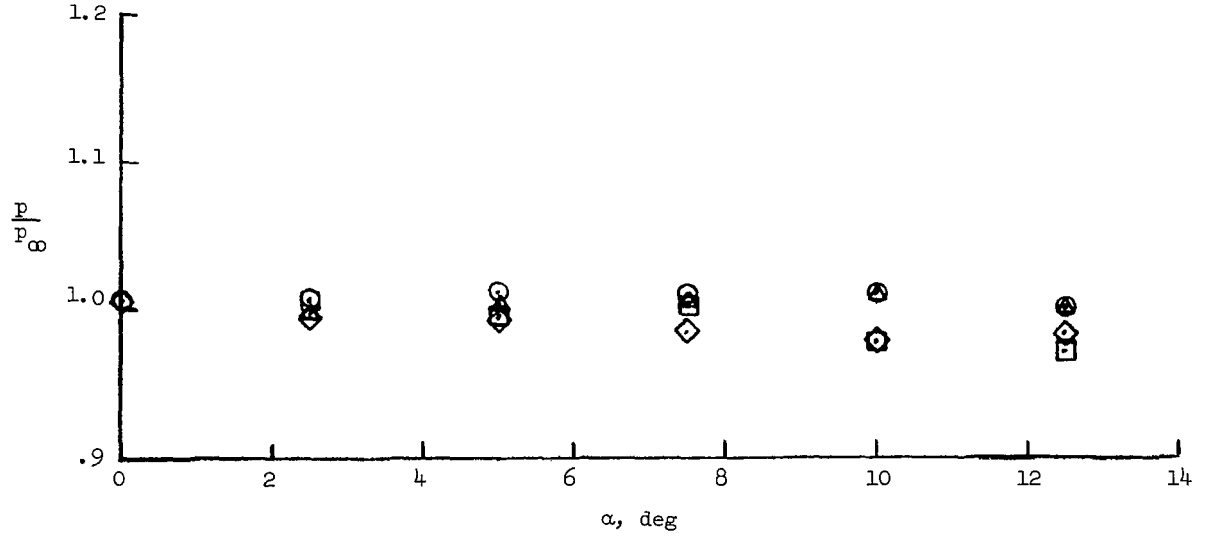

(b) $\omega = 3^{o}$; $M_{\infty} = 2.5$.

Figure 14.- Experimental calibration of static-pressure probes at angle of attack. Tip-cone half-angle, $\beta = 10^{o}$.

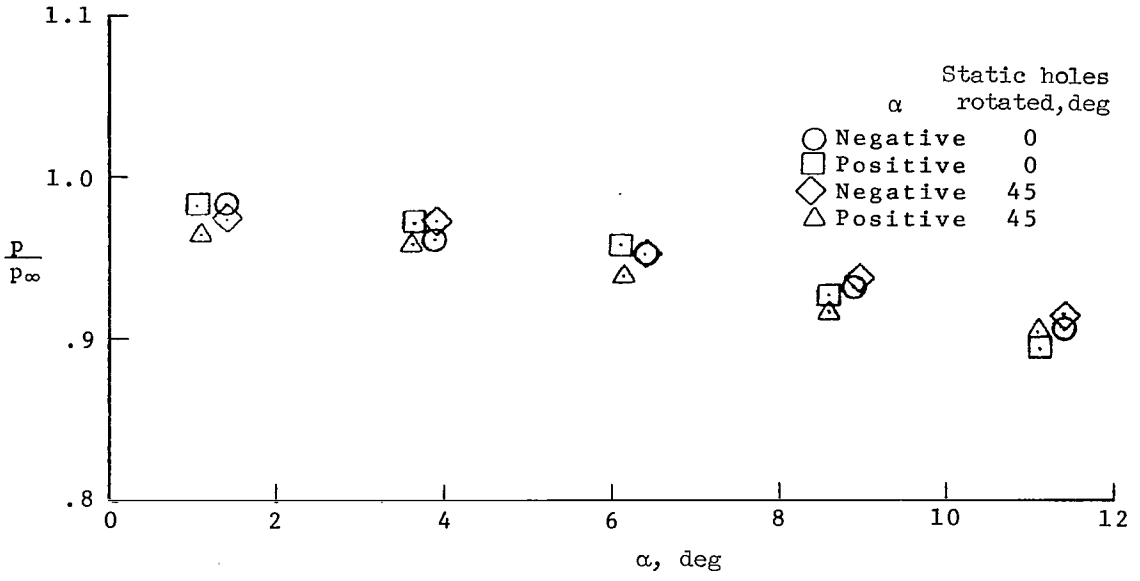

(c) $\omega = 2^{o}$; $M_{\infty} = 4.0$.

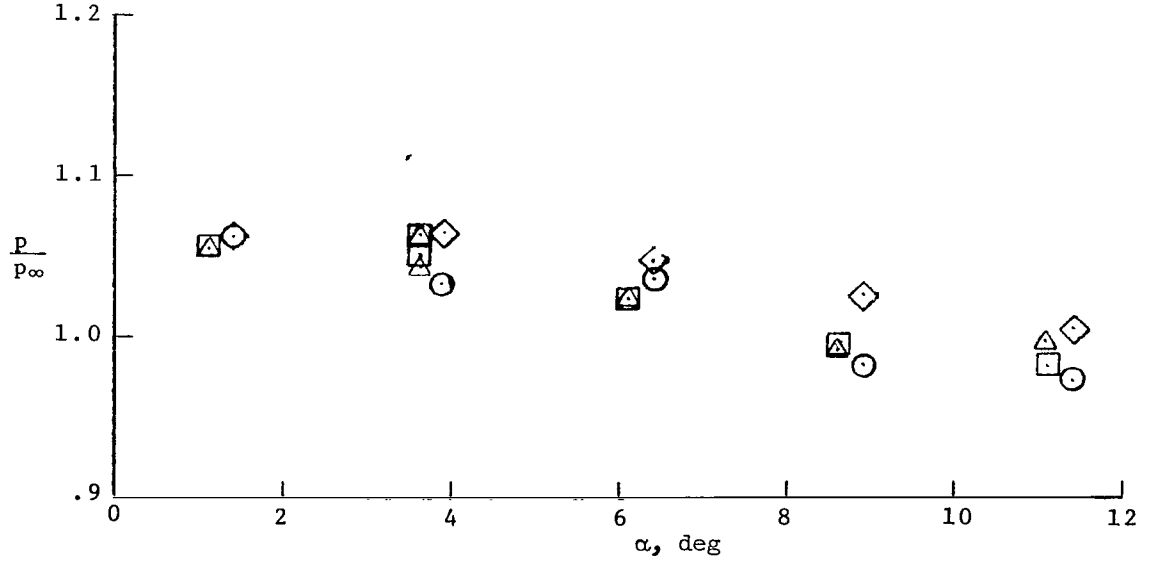

(d) $\omega = 3^{o}$; $M_{\infty} = 4.0$.

Figure 14.- Concluded.

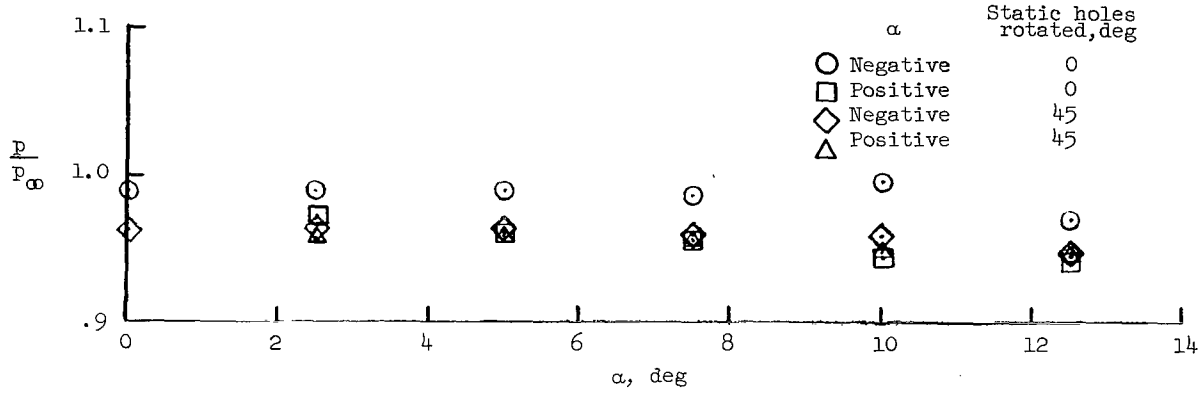

(a) $\omega = 2.0^{\circ}$; $M_\infty = 2.5$.

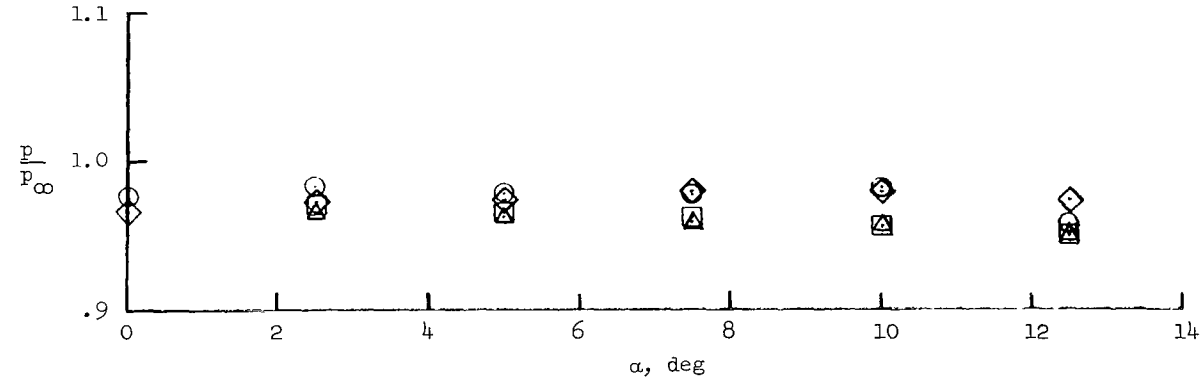

(b) $\omega = 3.5^{\circ}$; $M_\infty = 2.5$.

Figure 15.- Experimental calibration of static-pressure probes at angle of attack. Tip-cone half-angle, $\beta = 20^{\circ}$.

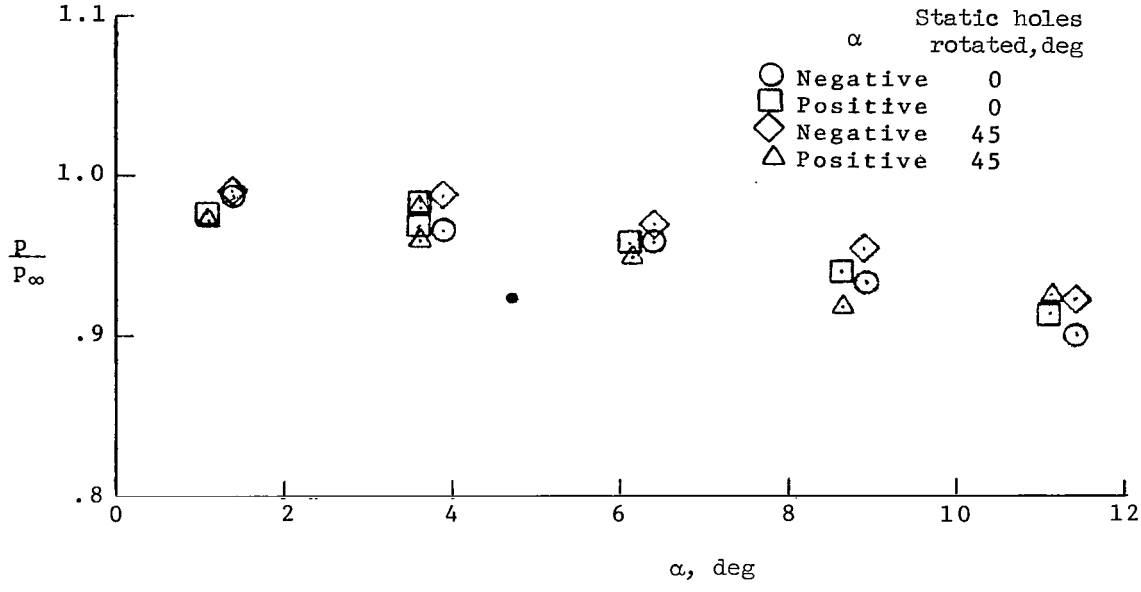

(c) $\omega = 2.0^{\circ}$; $M_{\infty} = 4.0$.

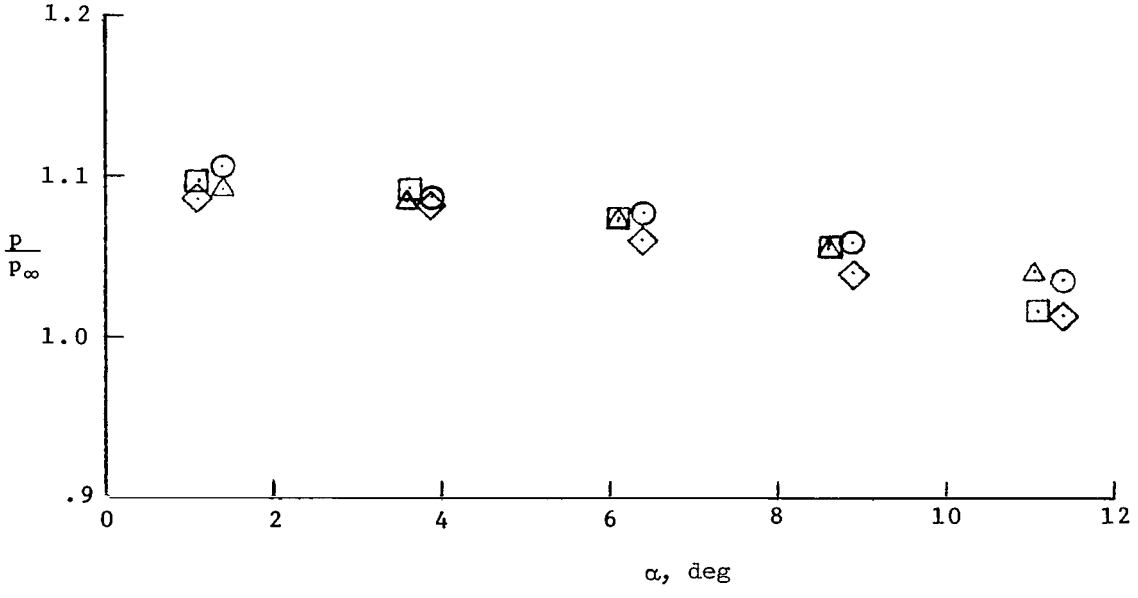

(d) $\omega = 3.5^{\circ}$; $M_{\infty} = 4.0$.

Figure 15.- Concluded.

"The aeronautical and space activities of the United States shall be conducted so as to contribute . . . to the expansion of human knowledge of phenomena in the atmosphere and space. The Administration shall provide for the widest practicable and appropriate dissemination of information concerning its activities and the results thereof."

—NATIONAL AERONAUTICS AND SPACE ACT OF 1958

NASA SCIENTIFIC AND TECHNICAL PUBLICATIONS

TECHNICAL REPORTS: Scientific and technical information considered important, complete, and a lasting contribution to existing knowledge.

TECHNICAL NOTES: Information less broad in scope but nevertheless of importance as a contribution to existing knowledge.

TECHNICAL MEMORANDUMS: Information receiving limited distribution because of preliminary data, security classification, or other reasons. Also includes conference proceedings with either limited or unlimited distribution.

CONTRACTOR REPORTS: Scientific and technical information generated under a NASA contract or grant and considered an important contribution to existing knowledge.

TECHNICAL TRANSLATIONS: Information published in a foreign language considered to merit NASA distribution in English.

SPECIAL PUBLICATIONS: Information derived from or of value to NASA activities. Publications include final reports of major projects, monographs, data compilations, handbooks, sourcebooks, and special bibliographies.

TECHNOLOGY UTILIZATION PUBLICATIONS: Information on technology used by NASA that may be of particular interest in commercial and other non-aerospace applications. Publications include Tech Briefs, Technology Utilization Reports and Technology Surveys.

Details on the availability of these publications may be obtained from:

SCIENTIFIC AND TECHNICAL INFORMATION OFFICE

NATIONAL AERONAUTICS AND SPACE ADMINISTRATION

Washington, D.C. 20546